

# The impact of sea ice retreat on the spring phytoplankton bloom over the Labrador Sea Baffin Shelf from 2003 to 2013

---

Jonathan Edward James Southwell

MSci Oceanography

ID: 24655651

May 2015

SOES6071

Supervisor: Dr Eleanor Frajka-Williams

Word Count: 9,989



## Abstract

---

I have investigated the climatology of the Baffin Shelf bloom in the Labrador Sea and related its variability to local sea ice dynamics. Motivation for this study stemmed from the critical ecological value spring blooms have on the Labrador Sea ecosystem. The onset of the Baffin bloom typically occurred around late-April, with variation in timing of up 30 days over the 11-year record from Aqua-MODIS satellite ocean chlorophyll, 2003-2013. Sea ice retreat typically occurred from early-March, with similar variations in timing compared to the spring bloom. Sea ice retreat was calculated from Nimbus-7 SMMR and DMSP SSM/I-SSMIS satellite derived sea ice concentration over the same study period.

Strong statistical correlations were found between the timing of sea ice retreat ( $t_{ice}$ ) and the onset of the Baffin bloom ( $t_{sb}$ ) from 2003 to 2013, where an average delay of 52 days existed between  $t_{ice}$  and  $t_{sb}$  each year. In this study,  $t_{ice}$  was defined as the time when Gaussian fitted annual sea ice concentration was at its maximum, and  $t_{sb}$  was defined as the first time chlorophyll exceeded its median +5% threshold, prior to its spring maximum. Specific retreat mechanisms thought to be inducing the bloom were critically assessed based on evidence from existing studies and common sense reasoning. This study suggests the timing of the Baffin bloom is controlled by light limitation due to sea cover. Haline stratification may also be important for bloom intensity and duration.

Previous investigations in the Labrador Sea have suggested the spring bloom is divided into two distinct biogeographical zones. Based on the observations here, this study suggests the Labrador Sea is in fact divided into three unique regions, where the Baffin bloom occurs later than central and north blooms. Due to the short, efficient nature of the Labrador Sea food chain, ice retreat induced primary production of the Baffin bloom may have both large and direct consequences for the success of secondary producers, who coincide their reproductive cycles with the spring bloom. Mismatches between primary and secondary producers could prove detrimental to the success of higher trophic levels, particularly under a trend of decreasing ice coverage in the future. Future work could focus on: (1) gaining a greater understanding on the ecological impact of ice-induced spring blooms and (2) identifying more broadly where these blooms may exist, with the aid of northern hemisphere  $t_{sb}$  and  $t_{ice}$  anomalies presented here.

## Acknowledgements

I would like to acknowledge my supervisor Eleanor Frajka-Williams who has been an inspiration since meeting her in 3<sup>rd</sup> year, and throughout my dissertation. Many thanks to Eleanor for her dedicated support, advice and enthusiasm.

Most of all, I am forever grateful to my parents for their tireless support, understanding and encouragement throughout my education, particularly in the final years of my MSci degree.

# Content

---

<b>1. Introduction</b>	<b>1</b>
<b>2. Background</b>	<b>4</b>
2.1. Conventional spring bloom theory	4
2.2. Sea ice in bloom development	6
<b>3. Data</b>	<b>9</b>
3.1. Satellite chlorophyll concentration	9
3.2. Satellite sea ice concentration	9
3.3. Photosynthetically Available Radiation (PAR)	10
3.4. Wind & air temperature	10
3.5. ETOPO2v2 bathymetry	11
<b>4. Methods</b>	<b>11</b>
4.1. Broad scale observations	11
4.2. Mini-box	12
4.3. Multi-transect	14
4.4. Correlation	15
4.5. Brief account of additional methods explored	16
<b>5. Results</b>	<b>17</b>
5.1. Spatial & seasonal variability of chlorophyll concentration	17
5.2. Spatial & seasonal variability of sea ice extent & retreat	19
5.3. Impact of sea ice retreat on chlorophyll concentration	22
5.3.1. <i>Preliminary observations</i>	22
5.3.2. <i>Results from mini-box method</i>	24
5.3.3. <i>Results from multi-transect method</i>	30
<b>6. Discussion</b>	<b>34</b>
6.1. Baffin bloom climatology & coupling with physical properties	34
6.2. Interannual variability of the bloom in relation to physical forcing	40
6.3. Impacts of sea ice retreat driven blooms on the Labrador Sea ecosystem	42
6.4. Method selection	44
6.5. Main limitations & future work	46
<b>7. Conclusion</b>	<b>49</b>
<b>8. References</b>	<b>51</b>

## List of Figures and Tables

---

### **Figures:**

**Figure 1:** Map of Labrador Sea, including isobaths and key regions of interest, *p. 2*

**Figure 2:** Physical and biological properties of the Marginal Ice Zone during sea ice retreat, *p. 7*

**Figure 3:** Map of Labrador Sea to show geographical location and extent of each of the main methods, *p. 13*

**Figure 4:** Time series of chlorophyll pixel availability from the confines of the mini-box method from 2003 to 2013, *p. 14*

**Figure 5:** Spatial time series composites of interannual variability in April-May chlorophyll concentration across the Labrador Sea from 2003 to 2013, *p. 18*

**Figure 6:** Interannual variability in the position of the sea ice edge in the Labrador Sea when ice extent is at its annual maximum from 2003 to 2013, *p. 19*

**Figure 7:** Spatial time series composites of interannual variability in sea ice retreat in the Labrador Sea from 2003 to 2013, *p. 21*

**Figure 8:** Time series of sea ice concentration and chlorophyll concentration from 65N, 58W over the Baffin Shelf from 2003 to 2013, *p. 22*

**Figure 9:** Average timing of peak chlorophyll, onset of the spring bloom, and timing of sea ice retreat in the Labrador Sea between 2003 and 2013, *p. 23*

**Figure 10:** Scatter plot comparing timings for the onset of the spring bloom and sea ice retreat from broad scale observation data in Fig. 9 over the Baffin Shelf, *p. 23*

**Figure 11:** Annual time series comparison of sea ice concentration, Gaussian fitted sea ice concentration, and chlorophyll concentration during winter-spring period over the Baffin Shelf from 2003-2013 (from Mini-Box method), *p. 25*

**Figure 12:** Scatter plot comparing timings for the onset of the spring bloom and sea ice retreat for 2003-2013 from mini-Box method, *p. 26*

**Figure 13:** Average of January-May wind direction composites (including wind speed) for the mini-box area from 2003 to 2013, *p. 28*

**Figure 14:** Time series of monthly 2 metre air temperature over the Baffin Shelf (mini-box area) from 2003 to 2013, *p. 29*

**Figure 15:** Hovmøller diagrams for chlorophyll concentration and sea ice concentration from combined transect of the multi-transect method from 2003 to 2013, p. 30

**Figure 16:** Annual time series comparison of sea ice concentration, Gaussian fitted sea ice concentration, and chlorophyll concentration during winter-spring period derived from multi-transect method for 2003-2013, p. 31

**Figure 17:** Scatter plot comparing timings for the onset of the spring bloom and sea ice retreat for 2003-2013 from multi-transect method, p. 32

**Figure 18:** Average cycle of photosynthetically available radiation (PAR) over the Newfoundland and Baffin Shelves for 2003-2013, p. 36

**Figure 19:** *Upper Panel:* open water fraction vs. chlorophyll concentration 2003 – 2013 over the Baffin Shelf. *Lower Panel:* open water fraction vs. abundance of chlorophyll 2001 – 2004 in Disko Bay, West Greenland [taken from Heide-Jørgensen et al. (2007), p.91], p. 41

**Figure 20:** Northern hemisphere latitudinal anomalies for the onset of the spring bloom and timing of sea ice retreat for 2003-2013, p. 48

## Tables:

**Table 1:** Interannual comparison of the onset of the spring bloom and timing of sea ice retreat (including statistics) for the mini-box method from 2003 to 2013, p. 26

**Table 2:** Summary of chlorophyll concentration and sea ice concentration during key timings for mini-box method from 2003 to 2013, p. 27

**Table 3:** April-May statistics of chlorophyll and sea ice concentration from the mini-box method, p. 29

**Table 4:** April-May statistics of chlorophyll and sea ice concentration from the multi-transect method, p. 33

## 1. Introduction

The spring phytoplankton bloom is one of the most dramatic large scale ecological events of our oceans. It generates a temporary surge in organic carbon that is critical to ecosystem productivity and the oceanic carbon cycle (Townsend et al., 1992). In temperate oceans such as the North Atlantic, the spring bloom is attributed to spring time shoaling of the mixed layer depth (MLD) and increasing irradiance (Sverdrup, 1953). In high latitude seasonally ice covered waters, the mechanisms responsible for the development of spring blooms are more complex. For a great part of the year, many Arctic and sub-Arctic shelves are covered by sea ice. The ice restricts the availability of solar irradiance, limits the development of stratification by solar heating, and inhibits wind-driven vertical mixing and shelf break upwelling (Carmack et al., 2004). I undertake the first seasonality study over the Baffin Shelf (around 65°N, 62°W), investigating the role of sea ice retreat on the Baffin bloom. Particular emphasis is placed on the climatology of the bloom in relation to other distinct areas of blooming in the Labrador Sea and wider Arctic regions.

The Baffin Shelf is located in the northern sector of the Labrador Sea, south of Baffin Island. The Baffin Shelf forms part of an extensive seasonal ice zone. Sea ice generally starts to appear in November. It extends progressively southward along the Labrador Shelf, and across the shelf break towards the central Labrador Sea. Even in light ice years, the coverage and density of sea ice over the Baffin Shelf is extensive. Ice over the shelf begins retreating around mid-March, although the timing can vary by up to 1 month between years. The central Labrador Sea remains ice free throughout each year, likely owing to persistent wind-driven mixing, upwelling, currents and deep water formation (Smith et al., 1990). Well-

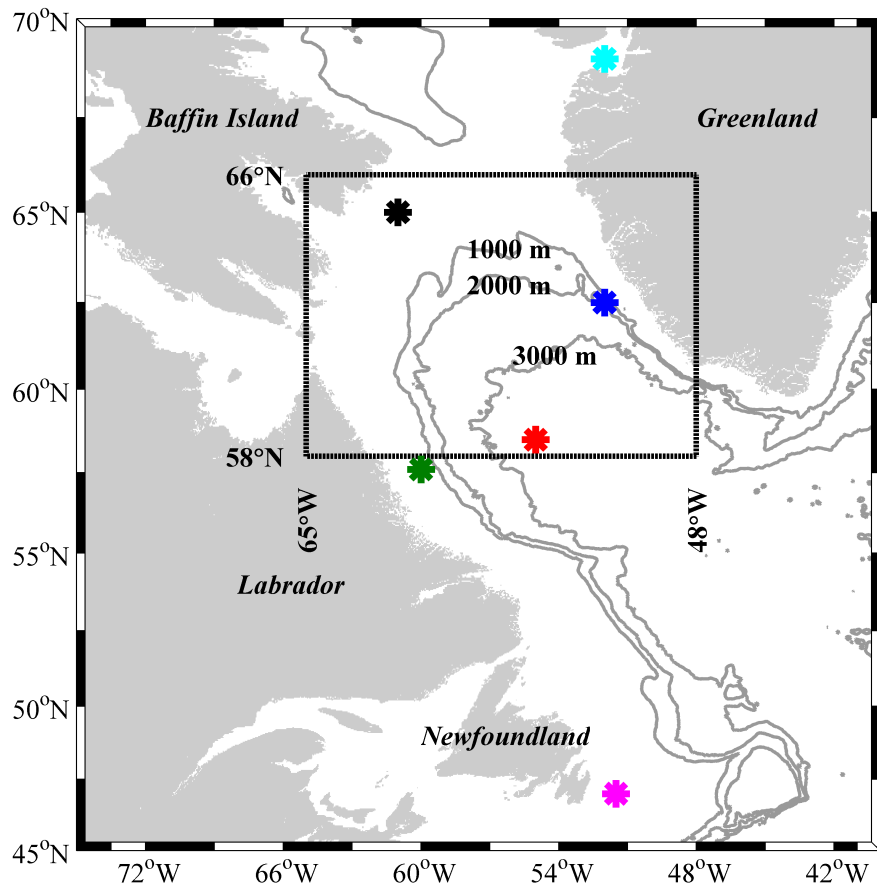


**Fig. 1.** Map of the Labrador Sea, including 1000, 2000 and 3000 m isobaths. Dashed box indicates approximate region of interest for sea ice-plankton study (58–66°N, 48–65°W). *Red dot:* Central Labrador Sea. *Blue dot:* North Labrador Sea. *Green dot:* Labrador Shelf. *Pink dot:* Newfoundland Shelf. *Black dot:* Baffin Shelf. *Cyan dot:* Disko Bay, Greenland.

mixed conditions and lack of usable light during winter prevents net growth of phytoplankton throughout the Labrador Sea (Barber & Massom, 2007). However, annual sea ice may be an important factor in the development of springtime conditions over the Baffin Shelf, potentially delaying the onset of the bloom. The annual bloom here develops around April-May and is relatively short-lived. Post-bloom production may be influenced by other factors, such as breakdown of haline stratification by wind shear, reintroducing nutrients to the surface (Heide-Jorgensen et al., 2007).

Research on ice-induced spring blooms in Arctic and sub-Arctic regions was difficult before the advent of long-term satellite chlorophyll records (Fischer et al., 2014). Now becoming increasingly available, they are essential to studying bloom dynamics in remote high latitude regions. A recent analysis of chlorophyll composites in the Labrador Sea by Frakja-Williams & Rhines (2010) revealed the spring bloom here could be divided into two distinct biogeographical zones (see Fig. 1) – the bloom in the central Labrador Sea being light limited and occurring later than the north bloom, which was attributed to offshore advection of freshwater from western Greenland. Wu et al. (2007) use a 7-year satellite time series of chlorophyll and sea ice concentration to identify a 0.96 correlation between the time of sea ice retreat ( $t_{ice}$ ) and the onset of the spring bloom ( $t_{sb}$ ) over the Labrador and Newfoundland shelves. They suggest melting of the sea ice increases upper ocean stability, promoting the ice-edge bloom.

Motivation for studying the role of sea ice retreat in high latitude spring blooms originates from the crucial influence these events have on the marine food web and community structure of Arctic ecosystems. Kahru et al. (2011) suggest climate change and large scale atmospheric processes such as North Atlantic Oscillation (NAO) and Pacific Decadal Oscillation (PDO) are responsible for a trend of earlier ice retreat and phytoplankton blooms in the Arctic. Models of Arctic food chains suggest changes in the timing of sea ice retreat is directly linked to the efficiency of energy transfer from bloom events to higher trophic layers (Hansen et al., 2002). Uncoupling this link may prove detrimental to the food web in its existing form (Kahru et al., 2011). Mismatches in the timing of ice retreat and the spring bloom may have particularly implications for the

Labrador Sea which contains a relatively short, efficient food chain (Pedersen & Kanneworf, 1995; Laidre et al., 2007, 2008). For example, the *Calanus* copepod graze directly on the phytoplankton (Head et al., 2000), and *Pandalus borealis* shrimp have adapted their reproductive cycle to match the timing of the annual phytoplankton bloom (Fuentes-Yaco et al., 2007).

Here I use 11 years of satellite chlorophyll and sea ice concentration observations (2003 to 2013) to investigate the role of sea ice retreat on the spring phytoplankton bloom over the Baffin Shelf. A variety of analysis methods are explored, to determine the timing of ice retreat ( $t_{ice}$ ) and the onset of the spring bloom ( $t_{sb}$ ). Specifically I have aimed to: (1) compare Baffin bloom climatology with existing key zones in the Labrador Sea; (2) test whether the retreat of seasonal sea ice causes the onset of the annual spring bloom using linear regression and correlations of  $t_{ice}$  and  $t_{sb}$ , in order to consider the underlying mechanism associated with sea ice retreat that may be responsible for the Baffin bloom.

## **2. Background**

### [2.1. Conventional Spring Bloom Theory](#)

A widely adopted explanation for the causation of the spring bloom is Sverdrup's 1953 critical depth hypothesis. Sverdrup defined the critical depth as the depth in the water column where vertically integrated production equals equivalent losses. Reducing wind shear, increasing solar radiation and available light towards spring leads to the MLD becoming shallower than the critical depth, allowing phytoplankton growth to exceed their losses, ultimately leading to the spring bloom (Sverdrup, 1953). His theory remained largely

unquestioned for more than sixty years, despite some studies highlighting the critical depth hypothesis could not explain all bloom formations in mid- to high-latitude ecosystems (Cushing, 1959; Yoder & McClain, 1993; Siegal et al., 2002). A long series of technological, theoretical and observational developments highlighted the potential pitfalls of Sverdrup's hypothesis (Fischer et al., 2014), namely: (1) growth is limited solely by light; (2) phytoplankton are well-mixed within the surface mixed layer; (3) loss rates remain constant with depth and time; (4) the ‘respiration’ term was the combination of several loss components, rather than being considered separately (Smetacek & Passow, 1990; Townsend et al., 1992; Eilertsen, 1993).

Two alternative mechanisms for the development of phytoplankton blooms have been put forward alongside Sverdrup's. The first mechanism is related to the vertical stability of the water column, where shoaling of the MLD from its winter maximum is not required for bloom initiation. Townsend et al. (1992) use in-situ depth profiles of chlorophyll florescence, irradiance and density in the Gulf of Maine to monitor biological activity in the water column prior to MLD shoaling. They found cell growth rates were supported by increasing solar elevation in spring, provided vertical mixing rates were low or the water column was neutrally stable. Similarly, Huisman et al. (1999) use a simple growth diffusion model (Okubo, 1980) to show a relaxation of turbulent mixing below a critical threshold allows a bloom to develop throughout the surface mixed layer if turbidity is low. Taylor & Ferrari (2011) also show that a weakening of turbulent convection can trigger the onset of the bloom in the North Atlantic, using in-situ meteorological products of atmospheric forcing. Chiswell (2011) uses satellite and in-situ measurements of chlorophyll alongside in-situ derived

measurements of MLD in the subtropical waters of New Zealand to establish the ‘Stratification-Onset Model’. He suggests the spring bloom develops in weakly stratified surface layers, created by the seasonal shutdown of turbulent mixing. His study highlights that phytoplankton are not evenly distributed within the mixed layer, as assumed by Sverdrup (1953).

The second mechanism, proposed by Behrenfeld (2010), uses satellite derived estimates of phytoplankton biomass to show net growth of phytoplankton in the North Atlantic can occur in winter when phytoplankton are diluted throughout the mixed layer. Behrenfeld (2010) suggests the dilution of phytoplankton reduces the number of interactions with prey, leading to fewer grazing losses. While the mixed layer is deep during winter, phytoplankton become temporally uncoupling with their grazers. Although growth rates during winter are low, loss rates as a result of dilution are lower still, enabling net positive growth and the onset of the bloom to occur.

## [2.2. Sea Ice in Bloom Development](#)

Early work in the late 1970’s suggested sea ice melting was responsible for spring bloom events in northern high latitudes, particularly those that occurred earlier or later than normal (Taniguchi et al, 1976; Schandelmeier & Alexander, 1981). This area of research builds on the existing theories described in Section 2.1, by considering an additional component - the biological and physical implications of sea ice cover. Figure 2 graphically demonstrates the basic physical characteristics of the water column near the sea ice edge. Sullivan et al. (2014) and Wu et al. (2008) show that meltwater from season ice melt

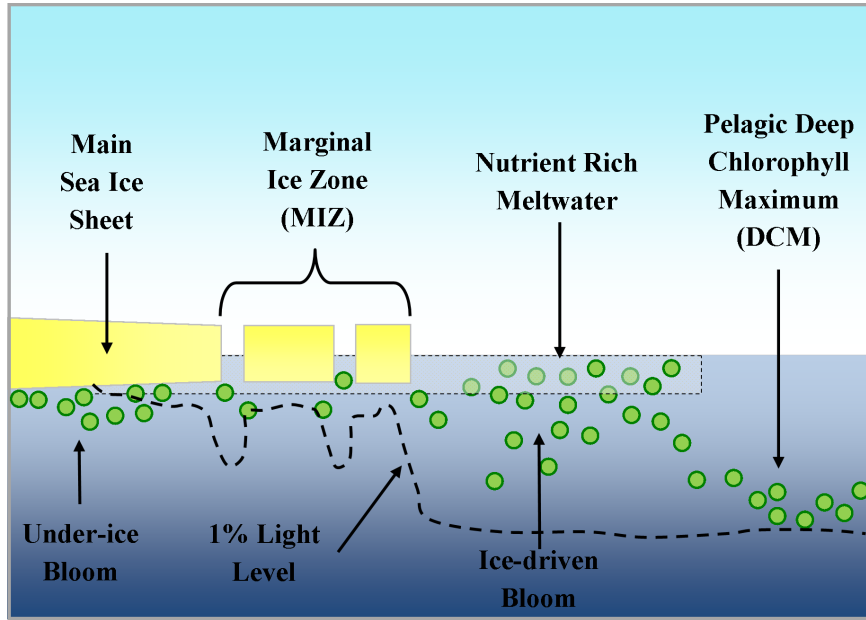


**Fig. 2.** Physical and biological properties of a theoretical Marginal Ice Zone (MIZ) during sea ice retreat. Green dots represent hypothetical distribution and density of phytoplankton cells.

generates a shallow mixed layer depth of 10-30 m. This thin band of sea ice meltwater is known to alter three components: (1) nutrient flux into the surface ocean, (2) availability of light, and (3) vertical mixing of the water column (Wang et al., 2014; Arrigo & van Dijken, 2004; Hunt et al., 2002).

As previously mentioned, Wu et al (2007) find a high correlation of 0.96 between the onset of the spring bloom and timing of sea ice retreat over the Newfoundland and Labrador shelves during their 7 year study. They suggest surface meltwater from sea ice promotes phytoplankton growth and the onset of the spring bloom. Sullivan et al. (2014) and Wu et al. (2008) come to similar conclusions for the eastern Bering Sea and Labrador Shelves. In contrast, Arrigo & Dijken (2004) find no such relationship in Cape Bathurst, Canada. Only the first year (1998) of the five year study shows an apparent coupling in ice-phytoplankton dynamics. Wu et al. (2007) also compare the timing of the event to other physical

parameters, such as air temperature ( $T_{air}$ ) and chlorophyll concentration duration ( $w$ ). They find the correlation for ice retreat to be the most significant, with the second and third largest being  $w$  and  $T_{air}$  at 0.90 and 0.73 respectively.

Heide-Jorgensen et al. (2007) compare the coupling of chlorophyll and sea ice in Disko Bay, West Greenland (see Fig. 1) in a 4 year study from 2001-2004. They show that coupling between phytoplankton and sea ice is bounded by an average open water percentage between 15-80%, which Heide-Jorgensen et al. (2007) speculate is likely due to combined availability of light and intensity of stratification due to surface meltwater.

Similar to pelagic blooms in ice-free regions, nutrients are important to ice-edge blooms. Wang et al. (2014) find iron to be a key nutrient for phytoplankton growth in the surface waters of high latitude systems, with its regime being strongly controlled by sea ice dynamics. Iron is captured and concentrated in sea ice during winter-time formation, following the replenishment of nutrients to the surface water column by seasonal convective overturning (Wang et al., 2014). Carmack et al. (2004) find that light limitation due to ice cover has the ability to control the timing of spring bloom production, but the availability of nutrients from ice meltwater and upwelling sets the limit in peak production. However, Ardyna et al. (2014) highlight that a lack of wind-driven mixing prevents the breakdown of haline stratification and supply of nutrients to the surface, eventually restricting production.

### **3. Data**

#### **3.1. Satellite Chlorophyll Concentration**

This report uses Level 3 mapped Aqua MODIS (MODerate-resolution Imaging Spectrometer) chlorophyll concentration at 8-day, 4 km resolution from the Ocean Color Database (<http://oceancolor.gsfc.nasa.gov/cms/>). Raw color measurements are converted to chlorophyll concentration using the OC3M empirical algorithm (O'Reilly et al., 2000), accounting for atmospheric interference, oceanic detritus and dissolved material. The final L3 mapped product has an estimated error of approximately 40% (Mahiny et al., 2013). Data used in this report spans from 2003 to 2013 for the Labrador Sea: 58°N to 66°N and 48°W to 65°W. (In this report, ‘chlorophyll’ and ‘chlorophyll concentration’ terms are used interchangeably).

#### **3.2. Satellite Sea Ice Concentration**

Sea ice concentration is created from brightness temperature data derived from Nimbus-7 SMMR and DMSP SSM/I-SSMIS passive microwave data, provided by the National Snow and Ice Data Centre (NSIDC) (<http://nsidc.org/data/polaris/>). A number of sensors are used to create this dataset: (1) Nimbus-7 Scanning Multichannel Microwave Radiometer (SMMR); (2) the Defence Meteorological Satellite Program (DMSP); (3) – F8, - F11 and – F13 Special Sensor Microwave/Imagers (SSM/I's); (4) DMSP-F17 Special Sensor Microwave Imager/Sounder (SSMIS). Corrections of sea ice extent and ice area between sensors is achieved by applying algorithm coefficients developed by the Laboratory for Hydrospheric Processes at NASA Goddard Space Flight Center (GSFC). Daily composites are provided on

a cylindrical projection at 25 km resolution. For this report, sea ice concentration data was re-worked to 8-day resolution to match satellite chlorophyll 8-day intervals. To achieve this, 8 individual daily files were averaged (according to individual grid points) to produce each 8-day composite. Sea ice concentration is given as percentage concentration from 0 to 100% (i.e. where 0% is open water). The data was also extracted for the Labrador Sea 58°N to 66°N and 48°W to 65°W for 2003 – 2013.

### **3.3. Photosynthetically Available Radiation (PAR)**

The Ocean Color Database also provided photosynthetically available radiation (PAR) from Aqua MODIS. 8-day composites from 2003 – 2013 were downloaded at 9 km resolution for the Newfoundland and Baffin shelves (47°N, 52°W & 65°N, 63°W respectively). Annual cycles of PAR were merged together to produce one average cycle at each site for the 2003–2013 spring period.

### **3.4. Wind & Air Temperature**

Monthly files of 10 metre wind speed (including U and V components) and 2 metre air temperature over the Baffin Shelf were sourced from ERA-Interim dataset, provided by the European Centre for Medium-Range Weather Forecasts (ECMWF). ECMWF monthly means from 2003-2013 are constructed from daily means. Data is used to relate the impact of air temperature and wind characteristics to the annual formation and breakup of sea ice over the Baffin Shelf. ERA-Interim is a global atmospheric reanalysis dataset from 1979 to present day. See Berrisford et al. (2011) for detailed documentation regarding parameters used in the dataset.

### 3.5. ETOPO2v2 Bathymetry

ETOPO2v2 is a 2-minute gridded global relief dataset provided by the U.S. National Oceanic and Atmospheric Administration (NOAA) National Geophysical Data Center (available from <http://ngdc.noaa.gov/mgg/global/etopo2.html>, as of 2006). The dataset is constructed from two main sources: (1) European Space Agency ERS-1 altimeter and US Navy Geosat altimeter measuring sea surface height and gravity anomaly; (2) in situ ship based echo soundings (Sandwell, 1991). The data is provided on cylindrical projection with a 2 x 2 minutes (3.7 x 3.7 km) resolution, with a vertical precision of 1 meter.

## 4. Methods

### 4.1. Broad Scale Observations

For broad scale observations of ice retreat ( $t_{ice}$ ) and onset of chlorophyll ( $t_{sb}$ ), chlorophyll required re-gridding to 25 x 25 km resolution to reduce the impact of cloudiness. All 4 km pixels within each new courser pixel were averaged to produce a new gridded concentration value. Estimates of  $t_{sb}$  were achieved by combining the 2003-2013 annual cycles of chlorophyll (according to day number) at each grid point to produce one average cycle for the study period. Due to the patchy nature of chlorophyll during the winter-spring period, estimates of  $t_{sb}$  could not be made for individual years at each grid point. Estimates of  $t_{sb}$  were calculated in two forms: (1) onset of chlorophyll (' $t_{sb}(onset)$ '), calculated as the first time when chlorophyll exceeds the median +5% threshold; (2) peak chlorophyll (' $t_{sb}(peak)$ '), calculated simply by finding the time when chlorophyll concentration is at its annual maximum. As well as re-gridding, chlorophyll was linearly interpolated from an 8-day

resolution, to a 1-day resolution using the *interp1* function in Matlab. Interpolating the time series did not change its visual appearance. Original data points were unaffected, while new data simply reduces the 8-day gaps to 1-day ones, retaining the original gradient of the line between 8-day points. Interpolation made no difference to the calculation of  $t_{sb}(peak)$ . However, due to the high growth rate of phytoplankton preceding the spring bloom, better representation of  $t_{sb}(onset)$  was achieved.

Unlike  $t_{sb}$  estimates, the lack of patchiness in sea ice data meant  $t_{ice}$  could be computed for each individual year at each grid point. All 11  $t_{ice}$  estimates (2003-2013) at each grid point were averaged to produce one  $t_{ice}$  estimate. For computational simplicity,  $t_{ice}$  was calculated as the day number when sea ice concentration fell to 50% of its annual maximum (hereafter denoted: ‘ $t_{ice}(50\%)$ ’), similar to the method used by Ji et al. (2013). Sea ice concentration was also interpolated to 1-day resolution to produce representative estimates of  $t_{ice}(50\%)$ .

#### 4.2. Mini-box

The mini-box is a 150,000 km<sup>2</sup> box covering 63-66°N and 58-62°W (see Fig. 3). Situated in the northern most area of the Labrador Sea, neighbouring Baffin Island, the selected region is situated over the Baffin Shelf covering a depth range of 50-1000 m.

Both the setup and execution of this method was designed for computational simplicity. For each 8-day time frame between 2003 and 2013, all chlorophyll and sea ice concentration pixels within the analysis box were averaged to produce a single mean value for each variable. For chlorophyll, this increased the yield of chlorophyll that may otherwise be missed due to cloudiness (see Fig. 4). Each year had an average of 48 8-day composites for

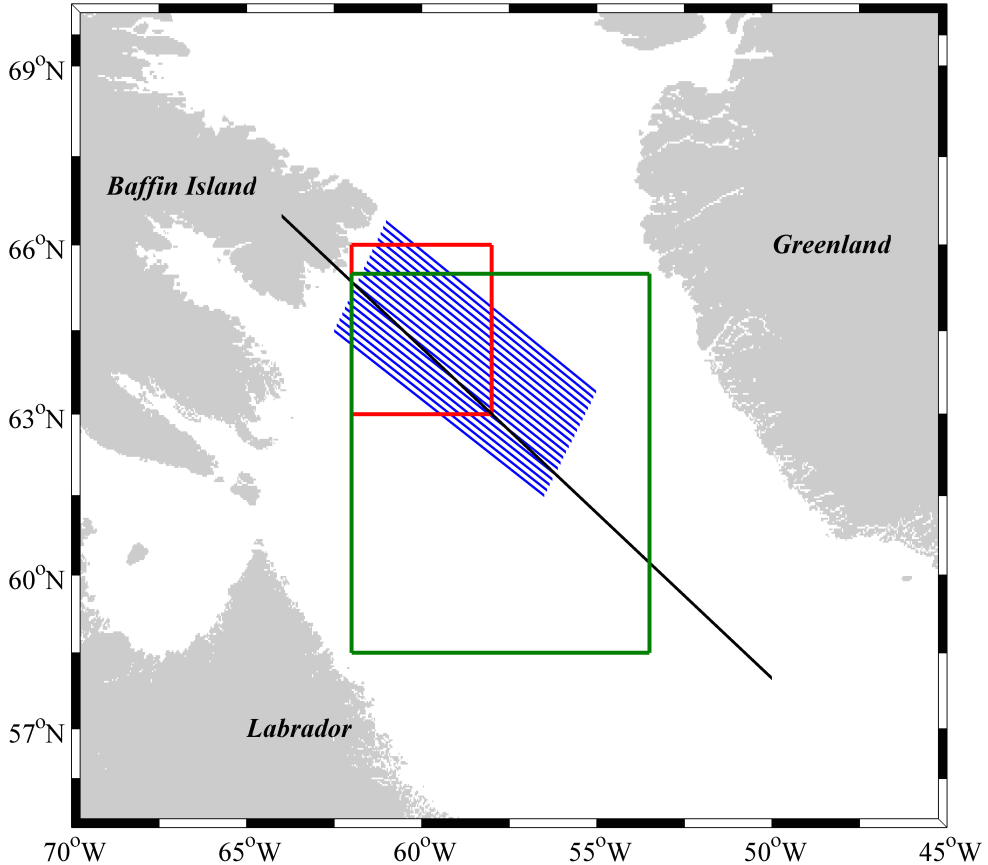


**Fig. 3.** Map of Labrador Sea to show the geographical extent of each of the main methods. (a) ‘Mini-box’ method (red), covering 63–66°N and 58–62°W. (b) ‘Multi-transect’ method (blue). First line starts 64.5°N, 62.5°W and ends 59.5°N, 52.5°W. Each subsequent line moves progressively northwards and eastwards in 0.2° intervals. (c) ‘Single transect’ method (black), from 66.5°N, 64°W to 58°N, 50°W. (d) ‘Large box’ method (green), covering 58.5–65.5°N and 53.5–62°W.

which averages could be taken. For each year, both variables were linearly interpolated onto a 1-day grid prior to further computations.

The annual cycle for sea ice concentration was clearly defined each year. However, concentration over shorter time scales (e.g. a monthly basis) was often erratic. Gaussian fitting was applied to the annual cycle of sea ice concentration to counteract this behaviour and produce representative estimates of  $t_{ice}$  (hereafter: ‘ $t_{ice}(Gaus)$ ’). The fitting type selected was 1 parameter non-linear least squares, using ‘bisquare’ robustness. Estimates for  $t_{ice}(Gaus)$  were calculated as the day number when fitted sea ice concentration was at its

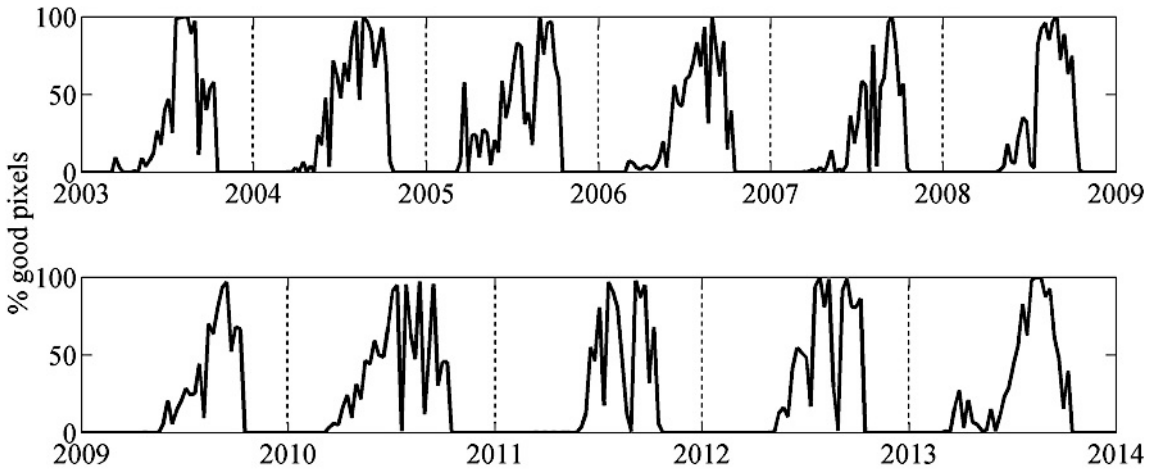


**Fig. 4.** Time series of chlorophyll pixel availability from the confines of the mini-box method ( $63\text{--}66^{\circ}\text{N}$  and  $58\text{--}62^{\circ}\text{W}$ ) from 2003 to 2013, where 0% indicates no chlorophyll pixels present, 100% indicates full coverage of chlorophyll data within the box.

maximum for each year. Estimates for  $t_{sb}(onset)$  were calculated as the first day when chlorophyll exceeded the median +5% threshold for each year. In similar studies, it is often common practise to ensure at least 3 chlorophyll data points exceed this threshold before the point of  $t_{sb}(onset)$  is declared. This was not necessary in this study, as the growth rate of chlorophyll during the spring growth phase was stable. Linear interpolation to a 1-day grid (as in Section 4.1) proved effective in producing representative estimates for both  $t_{sb}(onset)$  and  $t_{ice}(Gaus)$ .

#### 4.3. Multi-transect

A series of 20 transect lines parallel and within close proximity to each other were used to capture data over the Baffin Shelf (see Fig. 3). The lines run approximately perpendicular to both the ice edge and 1000 m and 2000 m isobaths. The first line starts at  $64.5^{\circ}\text{N}$ ,  $62.5^{\circ}\text{W}$  (near the Baffin Island coastline) and ends at  $59.5^{\circ}\text{N}$ ,  $52.5^{\circ}\text{W}$ . Each subsequent line moves progressively northwards and eastwards in  $\sim 0.2^{\circ}$  intervals. Employing multiple transects meant chlorophyll data could be captured over a wide spatial area, reducing the likelihood of

data being missed due to cloudiness. Along the length of each line, both chlorophyll and sea ice concentration is estimated at 4 km intervals. At each interval the four nearest pixels are linearly interpolated (using the ‘linear’ option in the Matlab *interp2* function) to produce one value. When fewer than four pixels are present, the ‘nearest neighbour’ option must be used instead due to restrictions in the *interp2* function. Once data for all 20 lines is collected, all lines are averaged together with respect to distance along the transect (where 0 km represents the most northerly position, nearest Baffin Island). To produce a time series of sea ice concentration and chlorophyll, all data along the combined transect is averaged for each time frame. To maintain consistency between methods, computation of  $t_{sb}(\text{onset})$  and  $t_{ice}(\text{Gaus})$  were carried out using the same method as in Section 4.2.

#### 4.4. Correlation

For broad scale observations, the mini-box, and multi-transect methods, linear regression analysis and correlation coefficients of  $t_{ice}$  and  $t_{sb}$  (irrespective of specific variant) were used to quantify the relationship between sea ice retreat and onset of the spring bloom (similar to the approach of Wu et al., 2007). Corresponding values of  $t_{sb}$  and  $t_{ice}$  for each year of the study were plotted on a scatterplot, with  $t_{ice}$  representing the x-axis and  $t_{sb}$  on the y-axis.

Simple linear regression (least squares) was computed using Matlab functions *polyfit* and *polyval* (see <http://uk.mathworks.com/help/matlab/ref/polyfit.html>). A simple Pearson product-moment correlation coefficient (R) was calculated using the *corrcoef* function in Matlab (see <http://uk.mathworks.com/help/ matlab/ref/corrcoef.html>) in order to quantify the degree of linear dependence between  $t_{ice}$  and  $t_{sb}$ , producing a value between -1 and 1. The *corrcoef* function is based upon the following equation:

$$R = R_{xy} = \frac{\sum_{i=1}^n (x_i - \bar{x})(y_i - \bar{y})}{\sqrt{\sum_{i=1}^n (x_i - \bar{x})^2} \sqrt{\sum_{i=1}^n (y_i - \bar{y})^2}}$$

where  $x$  and  $y$  are the two variables being compared ( $t_{ice}$  and  $t_{sb}$  respectively), of which there are  $n$  values. The parameters  $x_i$  and  $y_i$  refer to the set of  $t_{ice}$  and  $t_{sb}$  values respectively, and  $\bar{x}$  and  $\bar{y}$  is the mean of the  $t_{ice}$  and  $t_{sb}$  values respectively. The *corrcoef* function was also used to return p-values for testing the hypothesis of no correlation. The p-value is the probability of the observed correlation occurring due to random chance. For example, if  $p < 0.05$  then the correlation is significant at the 95% confidence interval.

#### 4.5. Brief Account of Additional Methods Explored

##### *Single Fixed Transect*

A fixed transect from 66.5°N, 64°W to 58°N, 50°W (see Fig. 3) was used to acquire chlorophyll and sea ice concentration for each 8-day frame in time from 2003 to 2013. Values for both variables are acquired at 4 km intervals along the transect line for each frame in time. At each interval, either ‘linear’ or ‘nearest neighbour’ is specified in the *interp2* function depending on the number of real data points available. This method was used due to its simple setup and approach. However, the combination of narrow transect width and cloud density during early spring each year meant the volume of useable chlorophyll data returned by this method was inadequate to allow computation of  $t_{sb}(onset)$ .

##### *Large Box*

The initial steps of this method are similar to those used in the mini-box method. A box from 58.5°N to 65.5°N and 53.5°W to 62°W (see Fig. 3) was used to produce a time series of

chlorophyll and sea ice concentration. At each 8-day frame in time, means of all chlorophyll and sea ice concentration pixels within the box were computed to produce a time series for each variable. Without the aid of further analyses, it was visually clear any calculations of  $t_{ice}(Gaus)$  or  $t_{sb}(onset)$  would not yield any statistically meaningful relationship as cycles in sea ice concentration and chlorophyll were not coupled interannually.

## 5. Results

### 5.1. Spatial & Interannual Variability of Chlorophyll Concentration

A spatial time series of interannual variability in chlorophyll concentration (April-May) is shown in Figure 5, showing the range and patterns of chlorophyll across the Labrador Sea. The greatest concentrations of chlorophyll, indicative of a bloom, are typically located over the 2000-3000 m isobaths, around 63°N, 52°W. The 2003 bloom appears particularly large and dense, while 2007 and 2010 blooms were more intense but more geographically restricted. Each year, blooming activity during the April-May period is concentrated off the west Greenland coast (except perhaps 2006). This activity is attributed to the advection of low-salinity water from west Greenland, which enhances stratification and allows phytoplankton to remain in the euphotic zone (Frajka-Williams & Rhines, 2010). Chlorophyll activity in the central Labrador Sea (around 57°N, 54°W) during April-May is significantly lower, typically  $< 0.5 \text{ mg m}^{-3}$ . Chlorophyll composites outside this period (not shown) show the bloom here to occur here between May and June, when the shutdown of turbulent convection allow phytoplankton to remain near the well-lit surface (Frajka-Williams & Rhines, 2010).

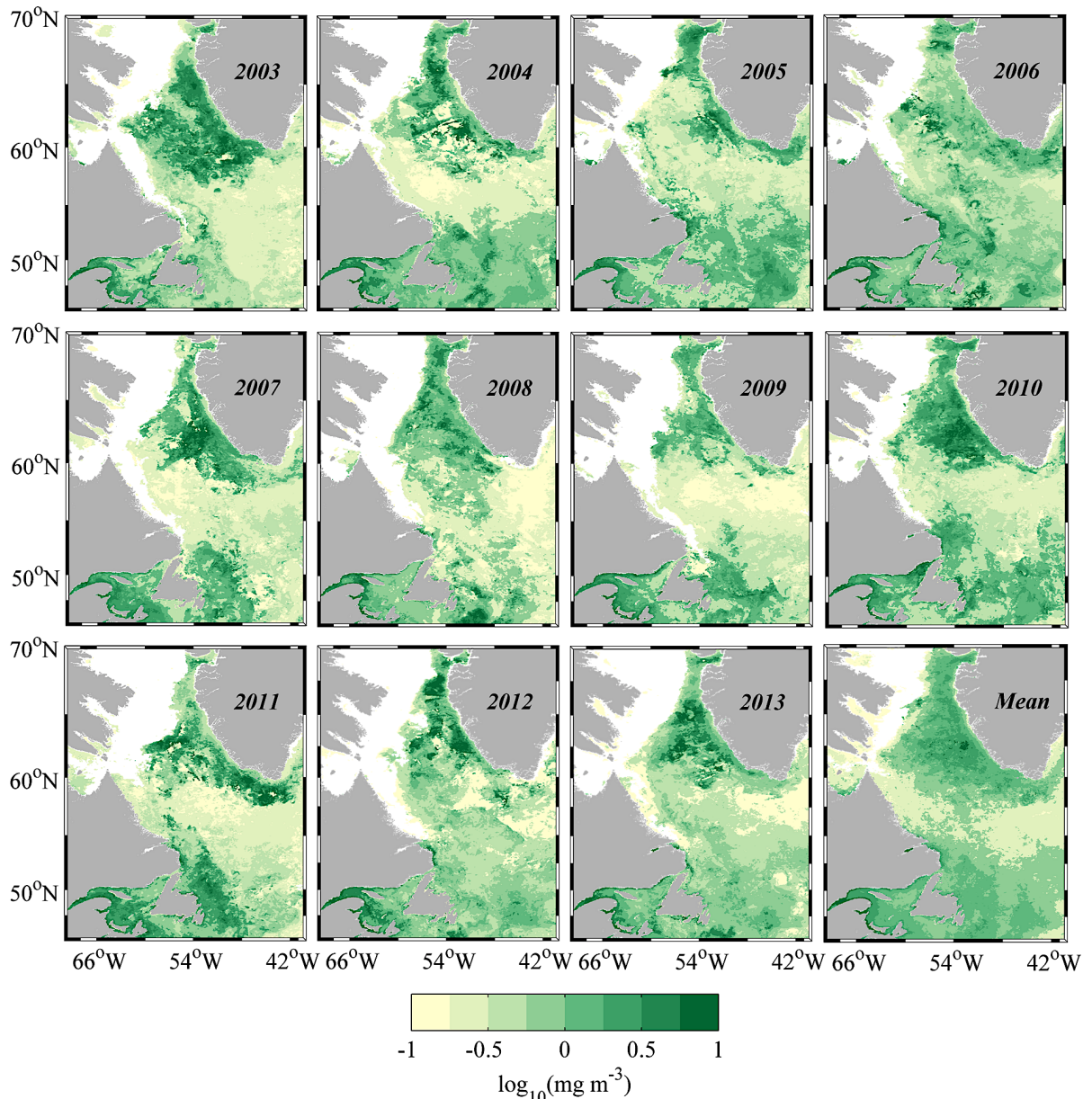


**Fig. 5.** Spatial time series composites of interannual variability of April-May chlorophyll concentration across the Labrador Sea, 2003-2013. Bottom-right panel shows average April-May chlorophyll concentration for all years, 2003-2013.

White areas in the panels of Figure 5 indicate the presence of sea ice, where the ice edge typically begins retreating during April. Compared to the magnitude and coverage of the north bloom, chlorophyll activity near the ice edge is harder to distinguish. However, during 2003, 2007 and 2011 chlorophyll concentrations  $> 2.5 \text{ mg m}^{-3}$  are easily identified within close proximity of the sea ice (see Fig. 5). Further, this activity extends along the majority of the northern section of the ice edge. Some regions of enhanced chlorophyll activity near

the ice edge are apparent during 2005, 2009, 2010, albeit significantly more localised compared to aforementioned years. It is unclear whether the observed activity near the ice edge is attributed to the presence of the ice, or the low-salinity surface water originating from West Greenland. In all other years, there is no obvious chlorophyll activity within a reasonable distance of the ice edge (e.g. 250 km).

## 5.2. Spatial & Interannual Variability of Sea Ice Extent & Retreat

A map of maximum sea ice extent from 2003 – 2013 is shown in Figure 6, where the maximum extent of the sea ice edge each year is indicated by the relevant contour. Maximum ice extent each year typically occurred during January or February. Sea ice along

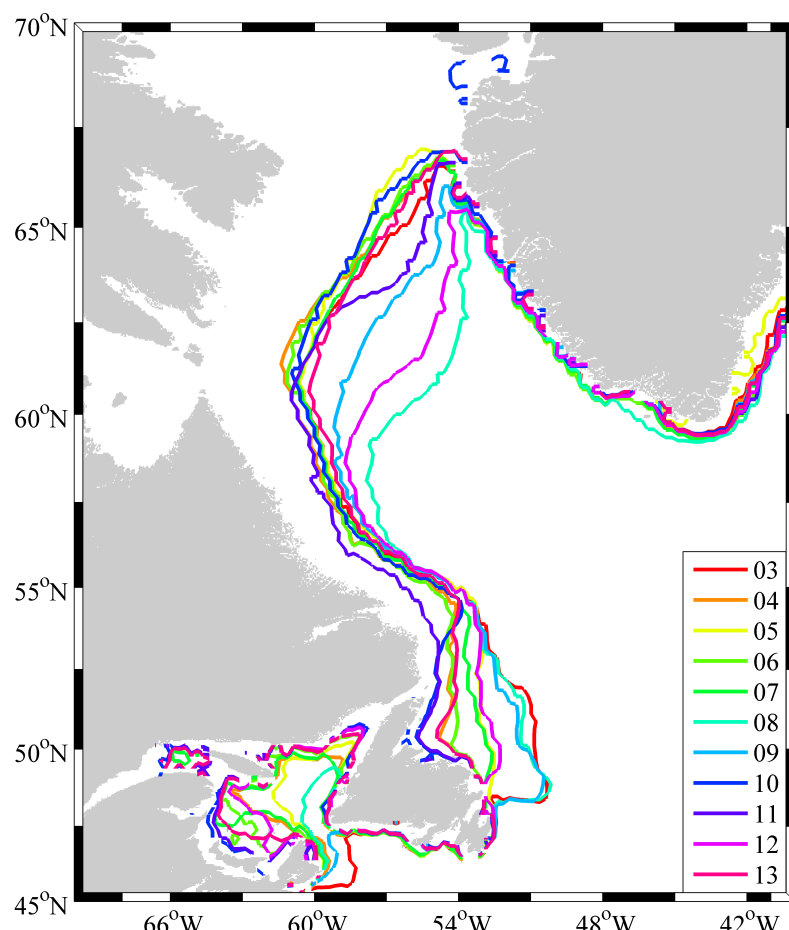


**Fig. 6.** Interannual variability in the position of the sea ice edge in the Labrador Sea when ice extent is at its annual maximum, 2003 - 2013.

the west coast of Greenland is confined to the coast, with limited offshore propagation. The greatest interannual variability in sea ice extent is observed south of Baffin Island (hereafter: ‘Baffin section’) where sea ice appears along the Island’s coastline from mid-December and propagates south-easterly towards the centre of the Labrador Sea. Here, the furthest south-easterly extent of the ice edge varies by up to ~775 km between minima and maxima years (January-February period of 2010 and 2008 respectively). For most years, the Baffin section extends no further than ~550 km from the Island’s coastline. The three biggest years in terms of maximum ice extent are 2008, 2009 and 2012, where the ice sheet extended much further into the Labrador Sea compared to other years. For example, the 2008 ice edge was ~1200 km from Baffin Island. Less variability in ice edge position is observed adjacent to the Labrador Shelf (hereafter: ‘Labrador section’). The Labrador section of the ice edge maintains an approximately uniform distance away from Labrador, following 1000 and 2000 m isobaths.

The spatial and seasonal variability of the sea ice was also analysed in terms of retreat time,  $t_{ice}(50\%)$  (see Fig. 7). The figure shows that during each year much of the outer ice sheet along Baffin and Labrador sections retreats simultaneously between day 80 and 100. Sea ice over the Labrador Shelf retreats no later than day 140-160 with the exception of some isolated localities during 2009 and 2013. During 2004, 2005 and 2011 the majority of the Labrador section of sea ice began retreating simultaneously around day 100 ( $\pm 20$  days). During 2003, 2007-2010, 2012-2013 retreat occurs over a slightly long time frame (up to 100 days), with ice nearest the Labrador coast retreating by day 180.

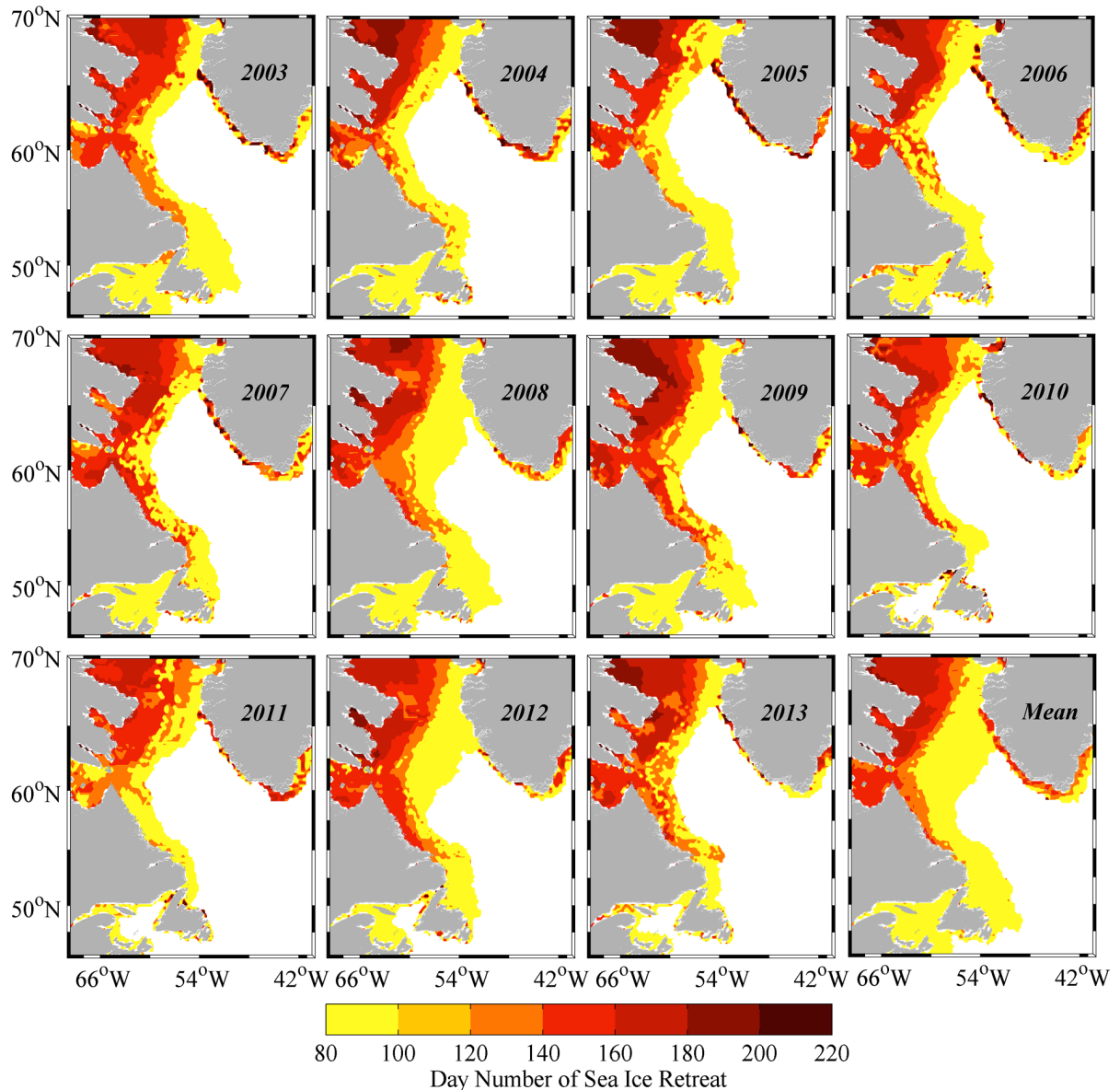


**Fig. 7.** Spatial time series of interannual variability in timing of sea ice retreat in the Labrador Sea, 2003-2013. Bottom-right panel shows average timing of sea ice retreat for all years, 2003-2013. White indicates areas of permanent open water.

The main mass of sea ice aft of the Baffin section ice edge generally retreats much later (after day 140) than the Labrador section, owing to its latitude. Figure 7 shows the latest retreat occurred in 2004, 2005 and 2009, where ice began retreating after day 200 (mid- to late-July), approximately 120 days (4 months) after maximum ice extent. Other years such as 2006, 2008 and 2013 were similarly late, despite affecting a much smaller proportion of the ice sheet (further north situated in the Davis Strait, around 68°N, 63°W). During 2003,

2010 and 2011 the majority of sea ice began retreating no later than day 160, with only isolated areas nearest the Baffin Island coast reaching day 180. This gave an average retreat time range of 80 days (~2.7 months) between the inner and outer extents of the ice sheet, compared to 120 days during late retreating years (e.g. 2009) - a difference of just over 1 month.

### 5.3. Impact of Sea Ice Retreat on Chlorophyll

#### 5.3.1. Preliminary Observations

A time series of chlorophyll and sea ice concentration from 65°N, 58°W over the Baffin Shelf is presented in Figure 8. Both variables exhibit clear seasonal cycles each year, where the onset of the spring bloom appears to follow the onset of sea ice retreat. Figure 9 shows how this trend was explored across a wider area of the Labrador Sea. From first glance, it is immediately obvious that  $t_{ice}(50\%)$  over the Baffin Shelf occurs at approximately the same time as  $t_{sb}(onset)$ , and approximately 40 days before  $t_{sb}(peak)$ . More generally, the bloom in this region occurs significantly later than the central bloom, whereas the bloom off west

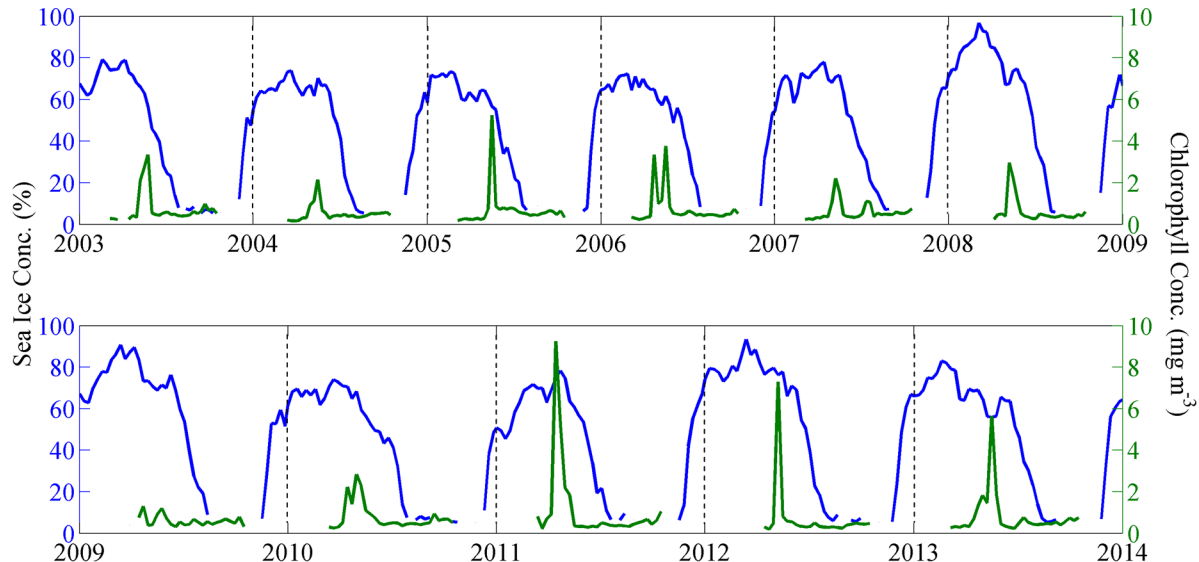


**Fig. 8.** Preliminary time series of sea ice concentration (blue) and chlorophyll concentration (green) from 65°N, 58°W over the Baffin Shelf, 2003-2013.

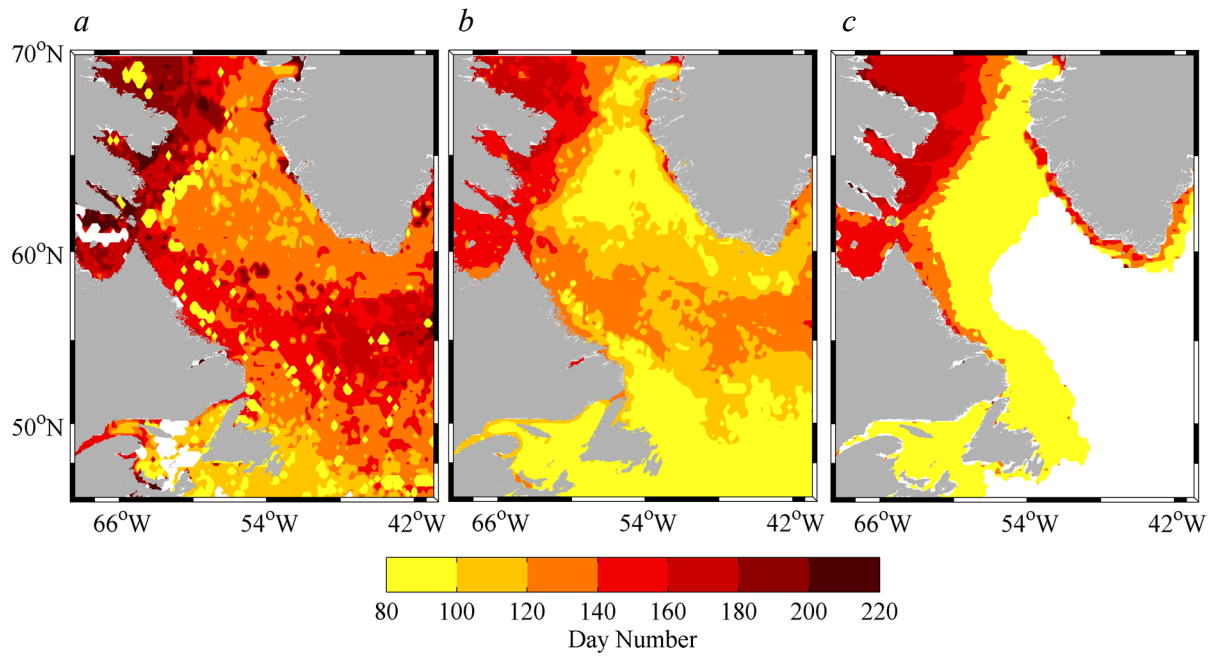


**Fig. 9.** (a) average timing of peak chlorophyll ( $t_{sb}(\text{peak})$ ), 2003-2013. (b) average start date of the bloom ( $t_{sb}(\text{onset})$ ), 2003-2013. (c) average timing of sea ice retreat ( $t_{ice}(50\%)$ ), 2003-2013. Note that timings of  $t_{sb}(\text{onset})$  over the Baffin Shelf (around 65°N, 58°W) are considerably later than other areas of the Labrador Sea, and are similar to  $t_{ice}(50\%)$  timings over the shelf.

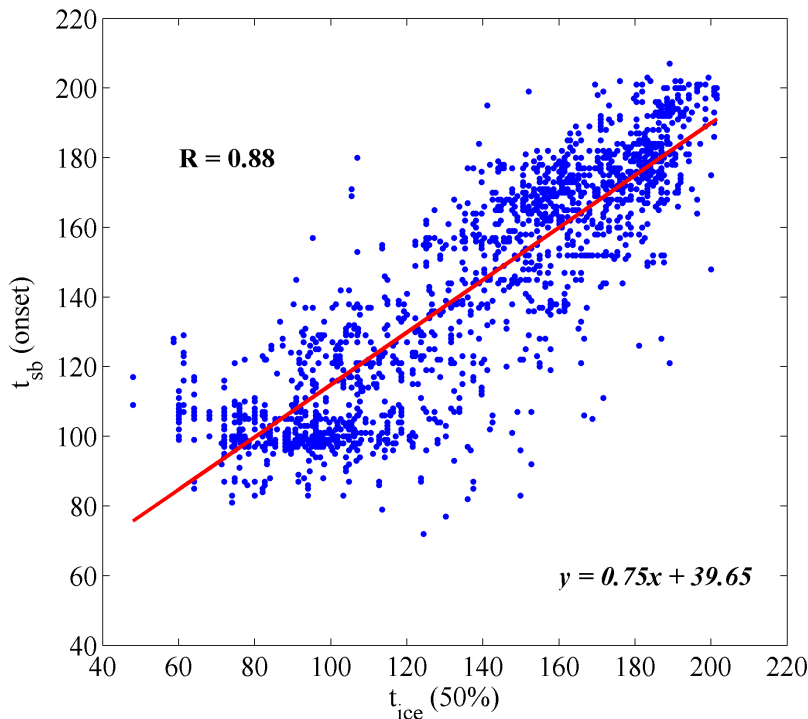


**Fig. 10.** Scatter plot comparing timings for the onset of the spring bloom ( $t_{sb}(\text{onset})$ ) and sea ice retreat ( $t_{ice}(50\%)$ ) from the relevant data in Fig. 9 over the Baffin Shelf. Red line is linear regression line with equation  $y = 0.75x + 39.65$ . Pearson correlation coefficient  $R = 0.88$ , significant at 99% confidence interval (based on 1937 samples).

Greenland (around 63°N, 52°W) occurs 40 days ( $\pm$  20 days) earlier than the central Labrador Sea (around 58°N, 54°W) despite being higher in latitude.

The relationship between  $t_{sb}(onset)$  and  $t_{ice}(50\%)$  at each grid point over the Baffin Shelf (60-70°N, 54-70°W) is demonstrated in Figure 10. The linear trend between  $t_{ice}(50\%)$  and  $t_{sb}(onset)$  is comparable to that found by Wu et al. (2007) offshore of Newfoundland (around 48°N, 51°W). The correlation coefficient of 0.88 produced a p-value of  $1 \times 10^{-5}$  (based on 1937 data points), showing correlation is significant beyond the 99% confidence interval which suggests there is a statistically significant trend between sea ice retreat and the onset of the spring bloom in this region. As a result of these preliminary analyses, the waters overlying the Baffin Shelf became the focal point for a more stringent investigation of sea ice-bloom dynamics.

### 5.3.2. Results from the Mini-box Method

Annual cycles of chlorophyll and sea ice concentration (including Gaussian fitting) for 2003 – 2013 from the mini-box method are presented in Figure 11. The chlorophyll cycles of 2004 and 2007 required linear interpolation to remove small gaps in the data (assumed to be caused by cloudiness, see Fig. 4). These patches were approximately 8-days in length due to the temporal scale of the satellite composites. Each composite is constructed from daily files, indicating cloud cover was persistent throughout the relevant 8-day periods. Interpolation was not used to complete the 2003 seasonal cycle as the temporal length of the patch after day 75 (48 days) was deemed too long for representative interpolation. Again, the large absence of data prior to the spring bloom was likely caused by persistent cloudiness following

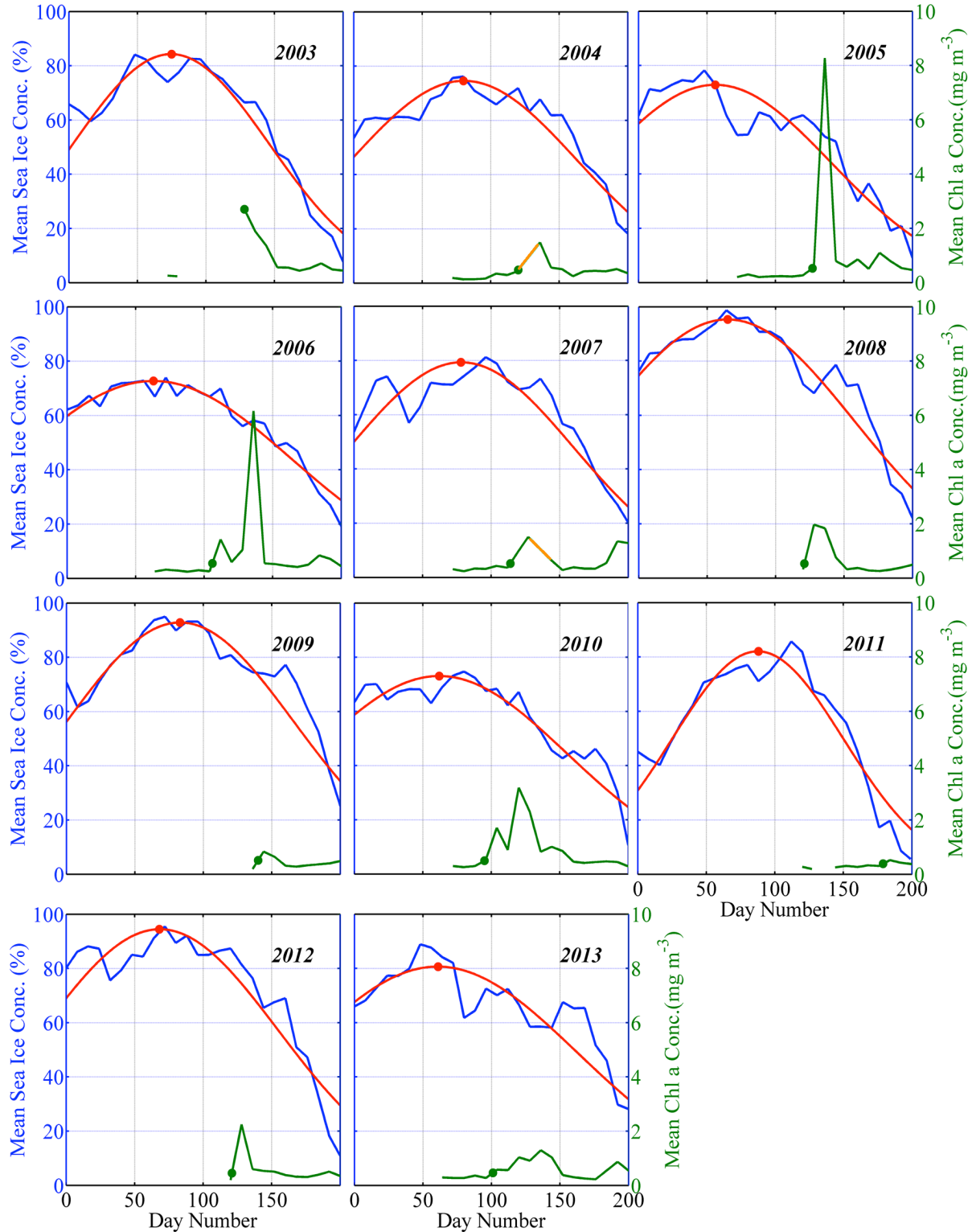


**Fig. 11.** Mini-box method: Annual time series comparison of sea ice concentration (blue line), Gaussian fitted sea ice concentration (red line), and chlorophyll concentration (green line) during winter-spring period over the Baffin Shelf, 2003-2013. Onset of the bloom ( $t_{sb}(onset)$ ) each year represented by green dot. Timing of sea ice retreat ( $t_{ice}(Gaus)$ ) each year represented by red dot. Sections of linear interpolation in 2004 and 2007 chlorophyll cycle highlighted in orange.

**Table 1.** Interannual statistical comparison of  $t_{ice}(Gaus)$  and  $t_{sb}(onset)$  timings (represented as day number) from the mini-box method, 2003-2013.

Year	$t_{ice}(Gaus)$	$t_{sb}(onset)$	Difference
2003	75	128	53
2004	80	120	40
2005	56	127	71
2006	63	106	43
2007	78	114	36
2008	65	121	56
2009	83	140	57
2010	62	95	33
2011	88	179	91
2012	68	121	53
2013	61	101	40
<i>Mean:</i>	70.82	122.91	52.09
<i>Standard Deviation:</i>	10.46	22.63	17.06
<i>Standard Error:</i>	3.15	6.82	5.14

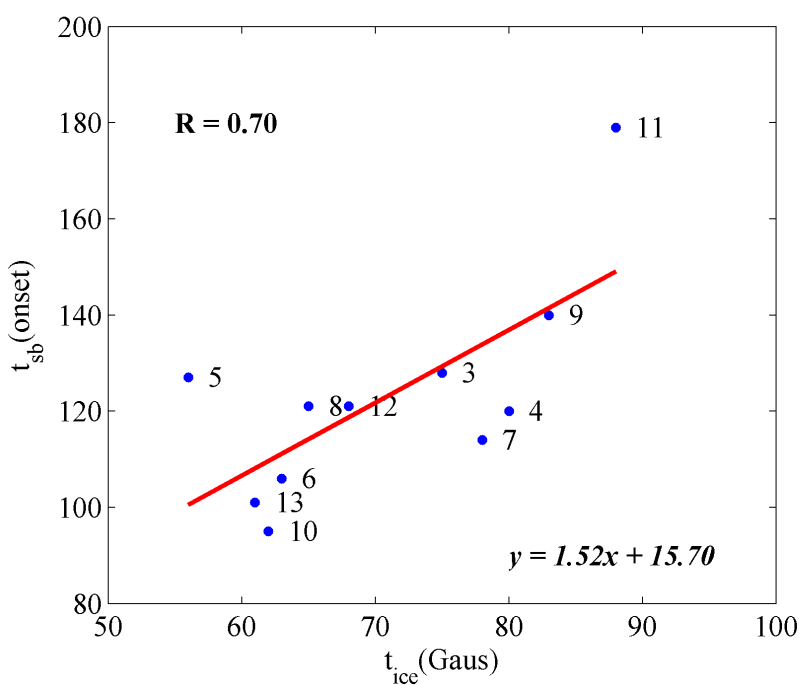


**Fig. 12.** Scatter plot comparing timings for the onset of the spring bloom ( $t_{sb}(onset)$ ) and sea ice retreat ( $t_{ice}(Gaus)$ ) as day number for 2003-2013 from the mini-box method. Red line is linear regression line with equation  $y = 1.52x + 15.70$ . Pearson correlation coefficient  $R = 0.7$  (all years except 2003), significant at 95% confidence interval (based on 10 samples).

the winter season. Computing a sensible estimate for the onset of spring growth and therefore timing of the spring bloom was not possible for 2003.

Springtime growth indicative of a bloom is apparent in all years, perhaps with the exception of 2009, 2011 and 2013. In fact, rescaling the chlorophyll axes of 2009, 2011 and 2013 panels (not shown) revealed a similar pattern of springtime growth compared to other years, albeit of lower magnitude. The onset of the spring bloom,  $t_{sb}(onset)$ , consistently occurring on average 52 days after  $t_{ice}(Gaus)$  each year (see Table 1). Timings of  $t_{ice}(Gaus)$  and  $t_{sb}(onset)$  each year are presented as a scatter plot in Figure 12. [The 2003 data point was excluded due to lack of chlorophyll data at the time of spring growth, despite producing timing estimates that complimented the linear trend]. With a high correlation coefficient of 0.7 (excluding 2003), this linear trend was significant at the 95% confidence interval, indicating that sea ice retreat may be responsible for the onset of the spring bloom. Bloom onset occurred earliest during 2010, where the magnitude of the bloom at day 120 was moderate compared to other years. During 2010,  $t_{ice}(Gaus)$  occurred at day 60, although this was not the earliest  $t_{ice}(Gaus)$  of the study period -  $t_{ice}(Gaus)$  during 2005 was earliest (day 53).

**Table 2.** Summary of chlorophyll concentration and sea ice concentration during key timings for mini-box method, 2003-2013. (\*not representative)

2003	2004	2005	2006	2007	2008	2009	2010	2011	2012	2013
<i>Sea ice conc. (%) at <math>t_{ice}(Gaus)</math></i>										
84	75	73	73	79	95	93	73	82	94	81
<i>Chlorophyll conc. (<math>mg\ m^{-3}</math>) at <math>t_{sb}(onset)</math></i>										
2.71*	0.49	0.53	0.55	0.51	0.53	0.51	0.49	0.39	0.45	0.46
<i><math>t_{sb}(peak)</math></i>										
128	135	136	136	127	128	144	120	184	128	137
<i>Chlorophyll conc. (<math>mg\ m^{-3}</math>) at <math>t_{sb}(peak)</math></i>										
2.71	1.44	8.27	6.16	1.49	1.97	0.83	3.18	0.52	2.25	1.26

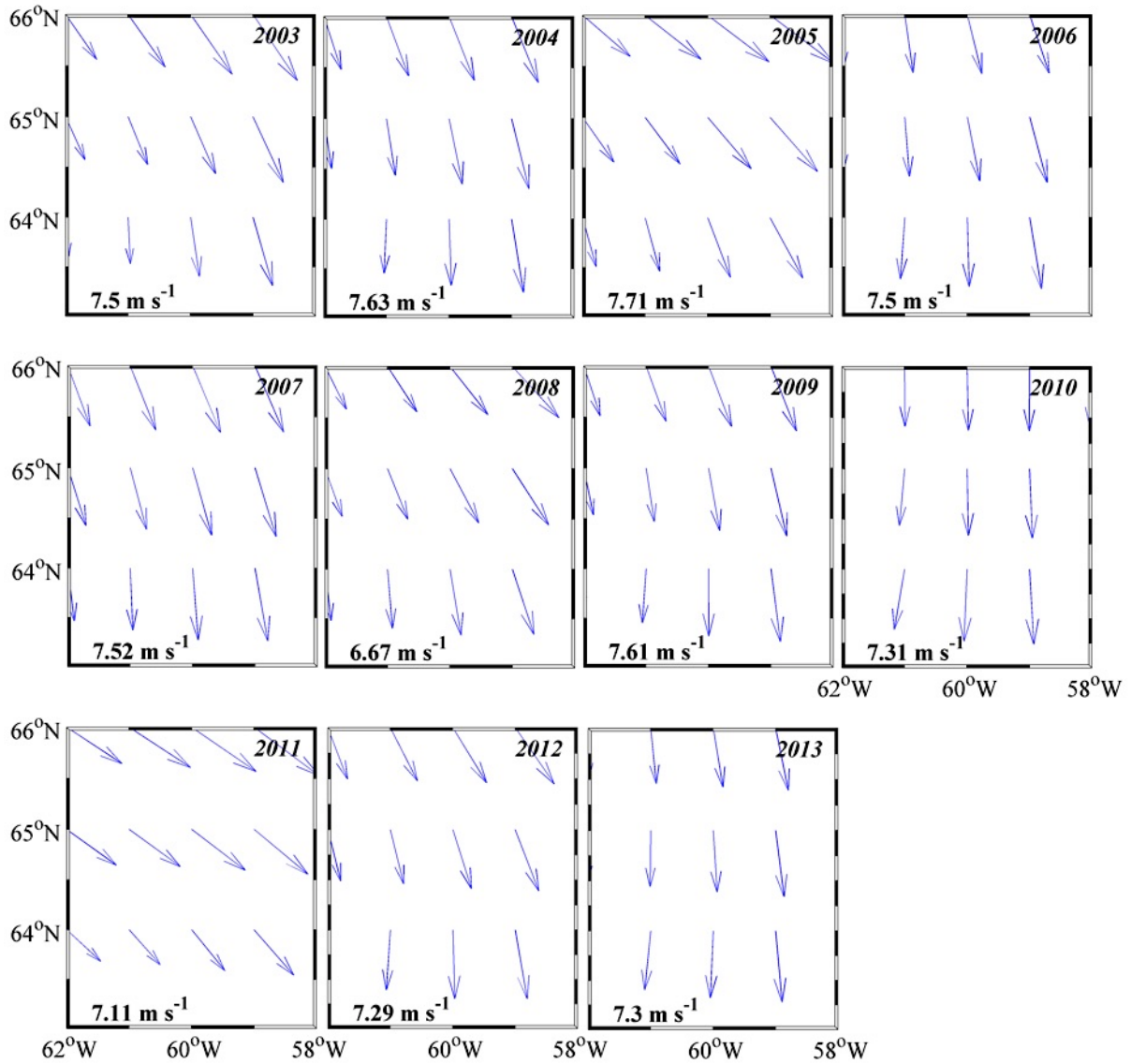


**Fig. 13.** Average of January-May wind direction composites (25 km resolution) for the mini-box area, 2003-2013. Wind speeds are spatial averages for the same period each year.

Interestingly, the 2005 bloom was the most intense at  $8.3 \text{ mg m}^{-3}$  (see Table 2) and had one of shortest periods between  $t_{sb}(\text{onset})$  and  $t_{sb}(\text{peak})$  (< 10 days). These observations coincided with the highest January-May average wind speeds ( $7.71 \text{ m s}^{-1}$ ) compared to other years (see Fig. 13). Wind direction during this period also had a stronger east component compared to most other years when wind direction was mainly south over the Baffin Shelf. Air temperatures were also notably greater compared to other years (see Fig. 14), where temperatures exceeded  $0^\circ\text{C}$  from day 52, 4 days before  $t_{ice}(\text{Gaus})$ . The 2005 data point could

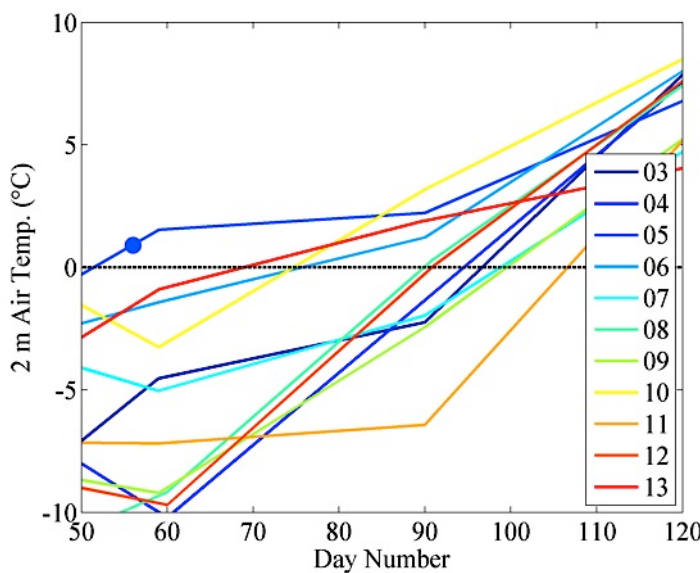


**Fig. 14.** Time series of monthly 2 metre air temperature over the Baffin Shelf, 2003-2013. Monthly composites (25 km resolution) for the mini-box area were spatially averaged to create the time series shown. Note how air temperature in 2005 exceeded 0°C on day 52, 4 days before  $t_{ice}(Gaus)$  that year (blue dot). Air temperature during day range 50-85 in 2005 was warmer than any other year.

**Table 3.** April-May statistics of chlorophyll and sea ice concentration from the mini-box method, 2003-2013.

2003	2004	2005	2006	2007	2008	2009	2010	2011	2012	2013
<i>Chlorophyll Concentration (<math>mg\ m^{-3}</math>)</i>										
<i>Mean</i>										
1.34	0.91	0.55	2.30	1.11	1.55	0.79	1.41	3.66	0.60	0.56
<i>Range</i>										
22.18	9.24	37.32	68.96	31.32	10.22	4.36	33.40	39.81	7.45	12.04
<i>Standard Deviation</i>										
2.44	0.92	1.85	5.60	1.41	1.33	0.42	1.85	10.18	0.53	0.53
<i>Sea Ice Concentration (%)</i>										
<i>Mean</i>										
68.4	59.9	41.3	54.4	67.6	83.1	84.1	54.4	72.5	83.7	64.1
<i>Range</i>										
100	100	98.6	100	100	100	100	100	99.6	100	100
<i>Standard Deviation</i>										
30.5	33.6	35.2	34.3	31.1	21.3	18.5	34.6	21.4	18.9	27.9

be regarded as an outlier, but did not adversely affect the trend between  $t_{ice}(Gaus)$  and  $t_{sb}(onset)$  as the aforementioned correlation shows. Timings of  $t_{ice}(Gaus)$  and  $t_{sb}(onset)$  for this year are further considered in the discussion section.

Statistics of chlorophyll and sea ice concentration during the April-May each year are provided in Table 3. This period corresponds to day numbers 91-151, when the onset of the bloom and peak chlorophyll occurred in all years except 2011.

### 5.3.3. Results from the Multi-transect Method

The time series of interannual variability in chlorophyll and sea ice concentration with respect to distance along combined transect is shown in Figure 15. The presence of sea ice is

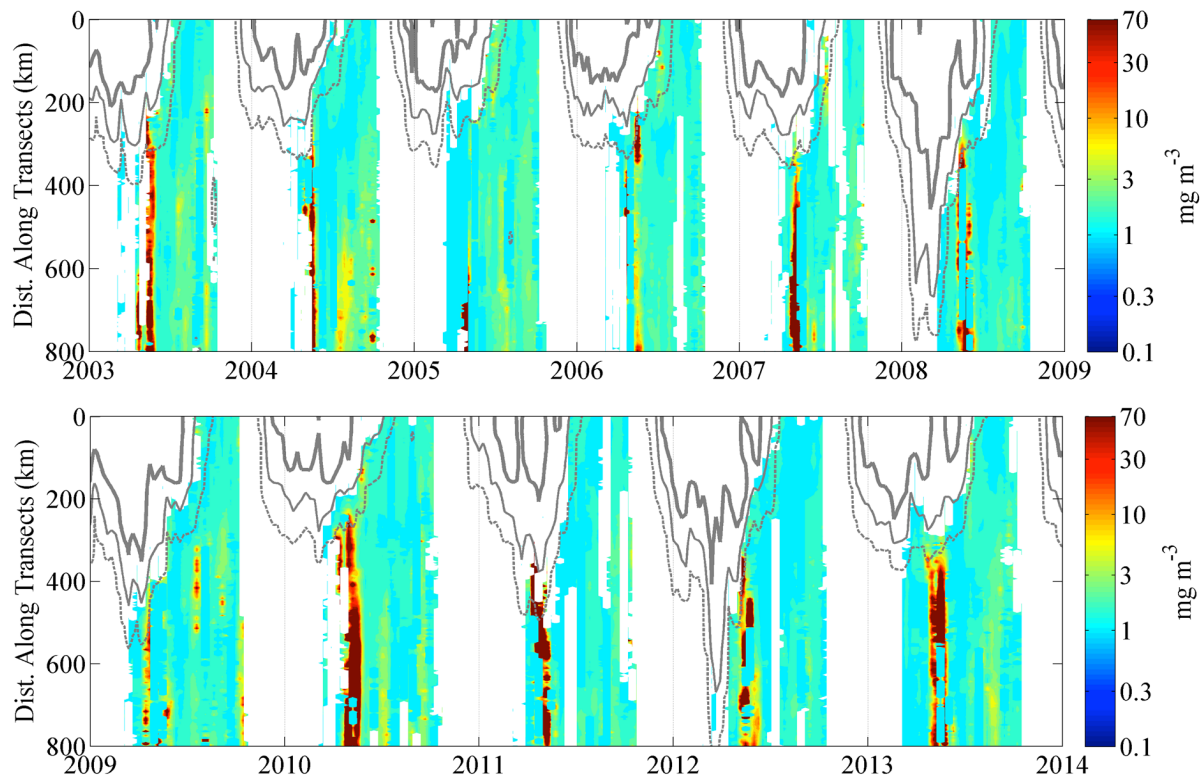


**Fig. 15.** Hovmöller diagrams of chlorophyll concentration and sea ice concentration from combined transect of the multi-transect method, where 0 km is situated over the Baffin Shelf and 800 km is towards the west coast of Greenland (see Fig. 3). Sea ice concentration represented by contours for 0% (dashed line), 30% (thin solid line), 60% concentration (thick solid line).

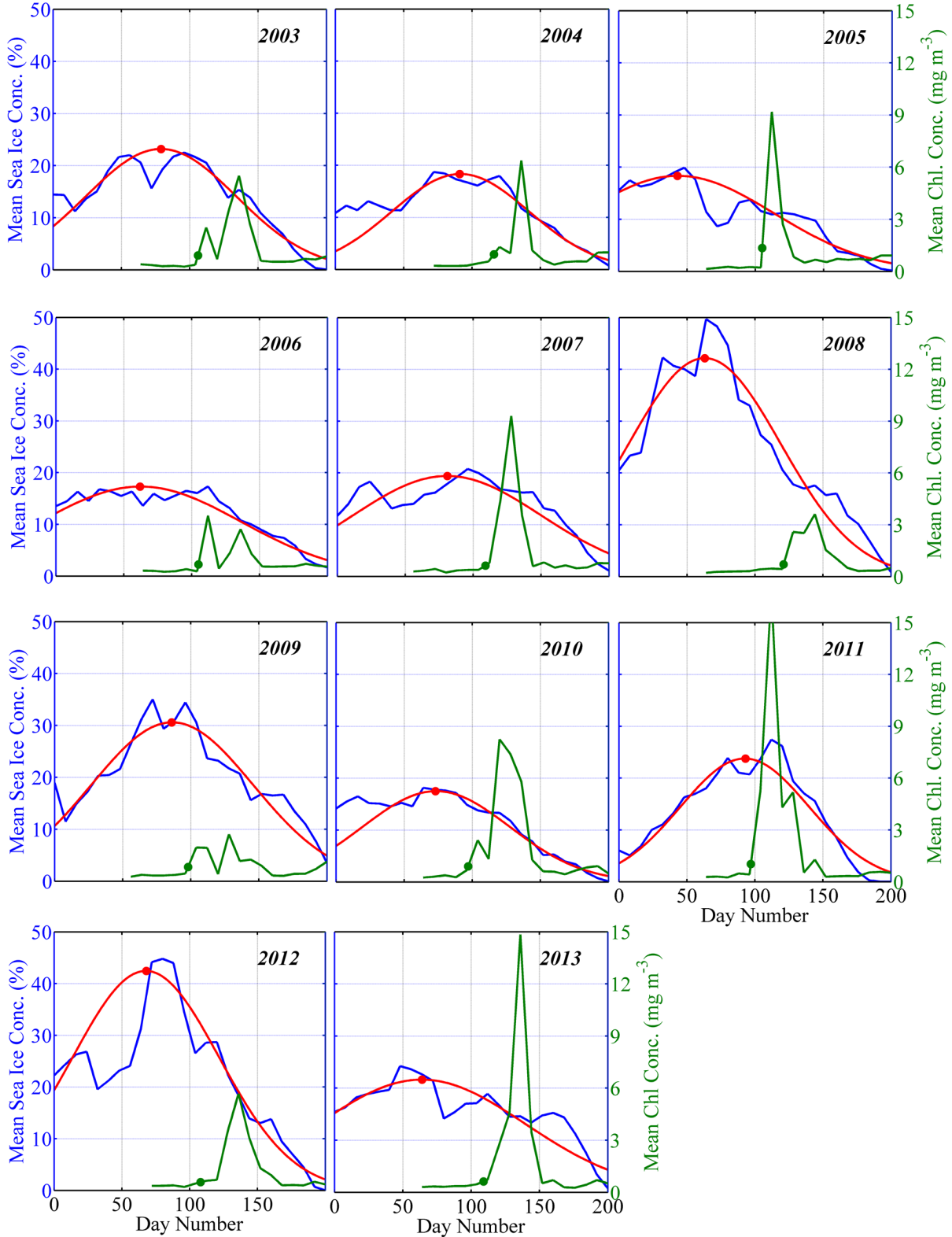


**Fig. 16.** Multi-transect method: Annual time series comparison of sea ice concentration (blue line), Gaussian fitted sea ice concentration (red line), and chlorophyll concentration (green line) during winter-spring period, 2003-2013. Onset of the bloom ( $t_{sb}(onset)$ ) each year represented by green dot. Timing of sea ice retreat ( $t_{ice}(Gaus)$ ) each year represented by red dot.

shown in the chlorophyll panel, where the number of chlorophyll pixels increase towards spring and with distance further south. The most intense chlorophyll activity each year occurs >300 km along the transect and south of the seasonal ice edge. The timing of peak chlorophyll is approximately uniform along the length of the transect, despite covering several degrees of latitude.

The 2010 bloom was strongest, with peak chlorophyll occurring close to the retreating ice edge. This bloom occurred in a less intense ice year, when both the spatial coverage and average concentration was slightly lower than most other years. Interestingly, chlorophyll is most intense near the ice edge during 2006, 2011, 2012, 2013 compared to further along the transect. During other years, activity along the transect is more uniform, with the exception of 2005 (a minor ice year) where spring time chlorophyll was weakest of all years, including

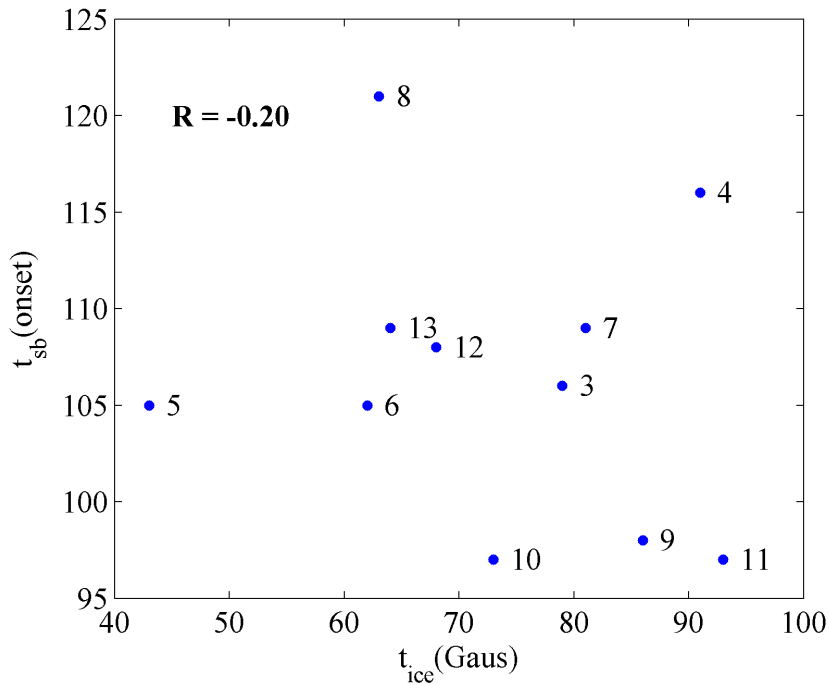


**Fig. 17.** Scatter plot comparing timings for the onset of the spring bloom ( $t_{sb}(\text{onset})$ ) and sea ice retreat ( $t_{ice}(Gaus)$ ) as day number for 2003-2013 from multi-transect method. Pearson correlation coefficient  $R = -0.2$  (not significant).

nearest the ice edge. Transect ice extent during 2008 and 2012 was particularly large but had limited bearing on the magnitude of blooms during these years. Sea ice concentration and chlorophyll data for each 8-day transect was averaged with respect to distance along the transect to produce the time series of each variable (including Gaussian fitting) for 2003 to 2013 (see Fig. 16). Figure 17 shows the comparison of  $t_{ice}(Gaus)$  and  $t_{sb}(onset)$  timings from Figure 16. Unlike using the mini-box method, no significant correlation was identified, implying that with this method, sea ice retreat does not influence the onset of the spring bloom. April-May statistics of chlorophyll and sea ice concentration for 2003-2013 from the multi-transect method are provided in Table 4.

**Table 4.** April-May statistics of chlorophyll and sea ice concentration from the multi-transect method, 2003-2013.

2003	2004	2005	2006	2007	2008	2009	2010	2011	2012	2013
<i>Chlorophyll Concentration (<math>mg\ m^{-3}</math>)</i>										
<i>Mean</i>										
2.20	2.07	0.97	1.42	3.04	1.35	1.20	3.50	3.39	2.18	2.20
<i>Range</i>										
49.78	18.54	65.41	19.52	36.50	8.79	24.13	50.65	40.16	46.02	53.41
<i>Standard Deviation</i>										
3.23	3.30	2.97	1.94	5.28	1.77	1.65	6.17	5.72	4.63	5.81
<i>Sea Ice Concentration (%)</i>										
<i>Mean</i>										
18.4	16.0	11.0	14.4	17.6	30.5	27.0	14.1	21.3	30.6	16.9
<i>Range</i>										
70.9	69.3	67.5	71.0	70.9	71.1	71.1	70.8	69.3	71.3	70.0
<i>Standard Deviation</i>										
26.7	25.2	21.2	23.8	26.6	29.2	29.6	23.8	26.1	28.3	24.8

## 6. Discussion

### 6.1. Baffin Bloom Climatology & Coupling with Physical Properties

This study has described the climatology of the Baffin Shelf bloom, with the mini-box method implying sea ice retreat does influence the timing of the bloom. Results from the multi-transect method contradict this, suggesting there is no coupling. For the purposes of this section and the following section, only the results from the mini-box method are considered, as it is deemed more appropriate for investigating sea ice and phytoplankton dynamics over the Shelf, mostly due to the spatial confinement of the analysis site. Reasons as to why the multi-transect and other methods did not produce a similar result to the mini-box method is discussed in Section 6.4.

Previous research has suggested the spring phytoplankton bloom in the Labrador Sea is divided into two distinct biogeographical zones, with the ‘north bloom’ (around 62°N, 52°W) occurring earlier than the ‘central bloom’ (around 58.5°N, 55°W) despite being higher in latitude (Frajka-Williams et al., 2009; Frajka-Williams & Rhines, 2010). By using simple correlations, Frajka-Williams & Rhines (2010) show the onset of the north bloom is largely attributed to the offshore advection of low-salinity water from Greenland ( $R = 0.8$ ), whereas the onset of the central bloom could only be correlated (albeit weakly) with irradiance ( $R = 0.5$ ). They show the north bloom occurs between April and May, and the central bloom during June. This study observed the Baffin Shelf bloom to occur between mid-April and late-June. Differences in bloom timing suggest the Baffin Shelf bloom is dynamically distinct compared to the other two regions.

The 2003-2013 time series here provides a wide range of ice-retreat timing and different responses from phytoplankton, thus allowing assessment of the correlation between sea ice and phytoplankton dynamics. The 11 year study period is significantly longer than many existing observational based sea ice-bloom studies, so the correlations identified here are perhaps more robust compared to those found by shorter studies. The mini-box method yielded a correlation of 0.7 between the timing of ice retreat and the timing of the spring bloom over the Baffin Shelf, significant at the 95% confidence interval. Based on conventional and sea ice bloom theory outlined in Sections 1 and 2, the timing of the Baffin bloom may be explained by the following hypotheses:

1. Timing is controlled by variations in light due to the annual cycle
2. Timing is controlled by variations in light, where sea ice retreat alleviates light limiting conditions
3. Timing is controlled by solar induced thermal stratification
4. Timing is controlled by haline stratification induced by sea ice meltwater
5. Or, inconclusive from data and analyses used here

Although these hypotheses were not directly tested in this study, the likelihood of each being true is carefully considered.

For the first hypothesis, it would be necessary to show that the availability of light during sea ice retreat is limiting for growth. If irradiance entering the surface water column were limiting for growth, a bloom would not occur even if sea ice had retreated. Over the Newfoundland and Labrador Shelves, ~15° south of the Baffin Shelf, Wu et al. (2007) found a correlation of 0.96 between the onset of the spring bloom and the timing of ice retreat.

Figure 18 shows a comparison of irradiance from the Newfoundland Shelf and the Baffin Shelf, where the onset of the spring bloom at each site is shown. All blooms from Wu et al. (2007) study period occur after day 70, whereas all blooms from this study period occur after day 95. Due to the seasonal progression of light with latitude, irradiance during these days is approximately 17 and 19 Einstein  $\text{m}^{-2}$  day $^{-1}$  respectively. Wu et al. (2007) suggests the shallow mixed layer from ice meltwater promoted the onset of the Newfoundland bloom, where light was not limiting to phytoplankton growth. Given the similar irradiance levels at both sites during the onset of blooms, light is unlikely to be controlling the timing of the Baffin bloom. This may also indicate that species composition, taxonomy and acclimation to light conditions is similar between sites at the time of the bloom (Staehr & Sandjensen,

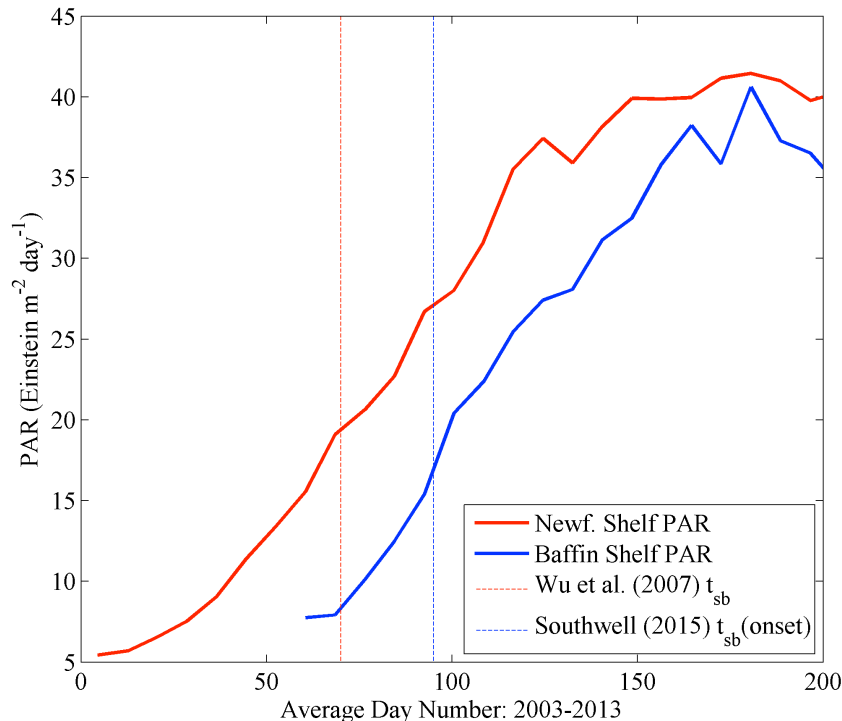


**Fig. 18.** Average cycle of photosynthetically available radiation (PAR) over the Newfoundland Shelf (around 47°N, 52°W) and Baffin Shelf (around 65°N, 58°W) for 2003-2013. Red vertical line represents the onset of the earliest spring bloom ( $t_{sb}$ ) over the Newfoundland Shelf (day number 70), from Wu et al. (2007). Average PAR over the Newfoundland Shelf during day number 70 is approximately 19 Einstein  $\text{m}^{-2}$  day $^{-1}$ . Blue vertical line represents the onset of the earliest spring bloom ( $t_{sb(onset)}$ ) over the Baffin Shelf (day number 95) from the mini-box method. Average PAR over the Baffin Shelf during day number 95 is approximately 17 Einstein  $\text{m}^{-2}$  day $^{-1}$ .

2005; Hickman et al., 2009). In a modelling study by Ji et al. (2013), their estimates for the timing of peak chlorophyll at 75°N in Baffin Bay are similar to our observational based estimates 10° further south. Unless phytoplankton species at 75°N in Baffin Bay are significantly better adapted to lower light conditions, this offers further indication that the timing of the Baffin bloom is not influenced by the annual cycle of light.

Assuming solar irradiance is sufficient for growth prior to the bloom, for the second hypothesis, it would be necessary to show that sea ice cover creates light limiting conditions. Seasonal sea ice and snow cover can reflect much of the incoming solar radiation due to its high albedo, coupled with high attenuation coefficient of the ice and snow, only a small fraction of light reaches the water beneath the ice sheet (Arrigo et al., 2012). In the seasonally ice-covered waters of the Beaufort Sea (around 74°N, 150°W), Arrigo & van Dijken (2004) and Carmack et al. (2004) show that light blocked by sea ice can be limiting to phytoplankton growth, delaying the onset of the bloom. However, during the ICESCAPE cruise in early July 2011, Arrigo et al. (2012) show that despite a less intense light regime beneath seasonal sea ice compared to neighbouring open water, an intense widespread under-ice bloom occurred over the continental shelf of the Chukchi Sea. The Chukchi Sea continental shelf is of similar latitude (around 68°N) to the northern Labrador Sea (around 65°N), and therefore subject to comparable surface irradiance levels during spring. These observations may suggest that irradiance beneath the Baffin Shelf ice sheet was not limiting to growth, providing the thickness and physical properties of the ice is comparable to that in the Chukchi Sea.

Using Sverdrup's critical depth model, Frajka-Williams & Rhines (2010) isolate the effect of MLD (World Ocean Atlas 2005) and light (SeaWiFS PAR) on the timing of the blooms in the Labrador Sea in three scenarios. In the first scenario, critical depths (a function of irradiance) were uniform, whilst annual cycles of MLD varied spatially across the Labrador Sea. In this case, the Baffin bloom was predicted to occur in early-March – much earlier than observations here. In the second scenario, MLD was kept uniform, but critical depth varied spatially according to the annual cycle of light. On this occasion the Baffin bloom was predicted around late June. When these two scenarios are combined, the bloom is predicted for mid-June, consistent with satellite chlorophyll observations presented here. The similarity in bloom start date between the second and combined scenarios would suggest light is responsible for delaying the bloom. Given that satellite PAR used in their critical depth calculations accounts for spatial variations in ice cover, this would suggest light limiting conditions delaying the Baffin bloom are a direct result of sea ice cover. Indeed, preliminary observations here (Fig. 9) highlighted the lateness of the spring bloom in areas of seasonal ice cover.

For hypothesis 3, thermally induced stratification is unlikely to be present at the time of the Baffin bloom as solar heat flux is relatively low. The magnitude of heat flux entering the surface water column at this time is probably too weak to shoal the MLD from its deep winter state (Sverdrup, 1953; Chiswell, 2011). The surface heat flux may be sufficient to induce weak stratification of surface layers (prior to MLD shoaling), although persistent convective overturning and turbulent wind shear following winter may prevent sustained formation required for a bloom (Chiswell, 2011; Taylor & Ferrari, 2011). Meltwater from sea ice could offer an alternative source of stratification, prior to thermal stratification

(hypothesis 4). Providing wind shear is below a threshold required for entrainment, low-salinity meltwater can enhance stratification of the surface water column, reducing vertical mixing of the water column (Zhang et al., 2010). With a reduction in mixing, phytoplankton may be held near the surface where they are able to exploit the iron supply from the melting sea ice, weak light and macro-nutrients (Taylor & Ferrari, 2011; Wang et al., 2014). Heide-Jorgensen et al. (2007) note that whilst a shallow meltwater layer from sea ice is key to the development of the Disko Bay bloom in west Greenland, the strong halocline and thermocline eventually limits growth once nutrients in the euphotic zone have been depleted (Nielsen & Hansen, 1999). The intensity of the Disko Bay spring bloom lasts up to a few weeks between the months of April and June (Juul-Pedersen et al., 2006; Heide-Jorgensen et al., 2007). Results here show the 2006 and 2012 Baffin Shelf spring blooms were particularly short-lived compared to other years, where haline stratification and finite supply of surface nutrients may have led to the rapid decline in chlorophyll. The 2005 bloom was also short-lived but its duration is not attributed to haline stratification (see Section 6.2).

As a result of Sverdrup's model, it was widely accepted that the spring bloom propagates from low to high latitudes shortly after the development of seasonal thermal stratification and increasing irradiance (Siegel et al., 2002). Spring bloom studies in the Labrador Sea (including this one) have shown this is not the case, with three areas of distinct blooms exhibiting varying dependence on stratification and light. This study suggests the timing of the Baffin bloom is strongly influenced by the timing of sea ice retreat due to ice-induced light limiting conditions. Haline stratification formed by ice meltwater may aid the development of the Baffin bloom, allowing phytoplankton to remain in the euphotic zone. The strength of this stratification may also set a cap on the duration and

productivity of the bloom, restricting the vertical flux of nutrients once finite supplies in the meltwater itself have been depleted.

## **6.2. Interannual Variability of the Bloom in Relation to Physical Forcing**

In Disko Bay, Heide-Jorgensen et al. (2007) find that years with late ice retreat attained slightly lower chlorophyll densities than years with early ice retreat. They also find the abundance of chlorophyll in light ice years was substantially greater compared to heavy ice years (in terms of open water coverage). In this study, the latest blooms (2004, 2009 and 2011) produced the lowest peak chlorophyll concentrations (1.44, 0.83 and 0.52 mg m<sup>-3</sup> respectively), consistent with Disko Bay observations. Figure 19 shows a comparison of chlorophyll concentration with open water fraction from this study and Heide-Jorgensen et al. (2007). Disko Bay coupling between chlorophyll and sea ice was bounded by an average open water fraction between 50 and 80%. This is similar to the Baffin Shelf where the main chlorophyll activity occurs between 60 and 90%. Heide-Jorgensen et al. (2007) suggest the combined effect of stable open water and availability of light is responsible for the observed trend in Disko Bay. The similarities between studies would suggest interannual changes in light climate due to ice cover over the Baffin Shelf can influence both the timing and the magnitude of the bloom here.

Sea ice retreat occurred earliest in 2005 over the Baffin Shelf (Fig. 12, Table 1). Despite the strong correlations found by this study, the onset of the bloom in 2005 occurred 71 days after ice retreat on day 127, 19 days longer than the average delay of 52 days. To adhere to the general trend observed from other years, the spring should have occurred around day 95 ± 15 days. During their short 4 year study, Heide-Jorgensen et al. (2007) find no evidence

of delay to the spring bloom in early ice retreat years, somewhat contrary to observations here and in the Bering Sea (Stabeno et al., 2001). Similarly, Wu et al. (2007) show early ice retreat over the Newfoundland and Labrador Shelves can lead to an early and prolonged spring bloom. Therefore, changes to the physical environment may be responsible for the late Baffin bloom in 2005. Tables 2 & 3 show how sea ice concentration during 2005 was particularly low compared to most other years. Wind speeds during the winter to spring

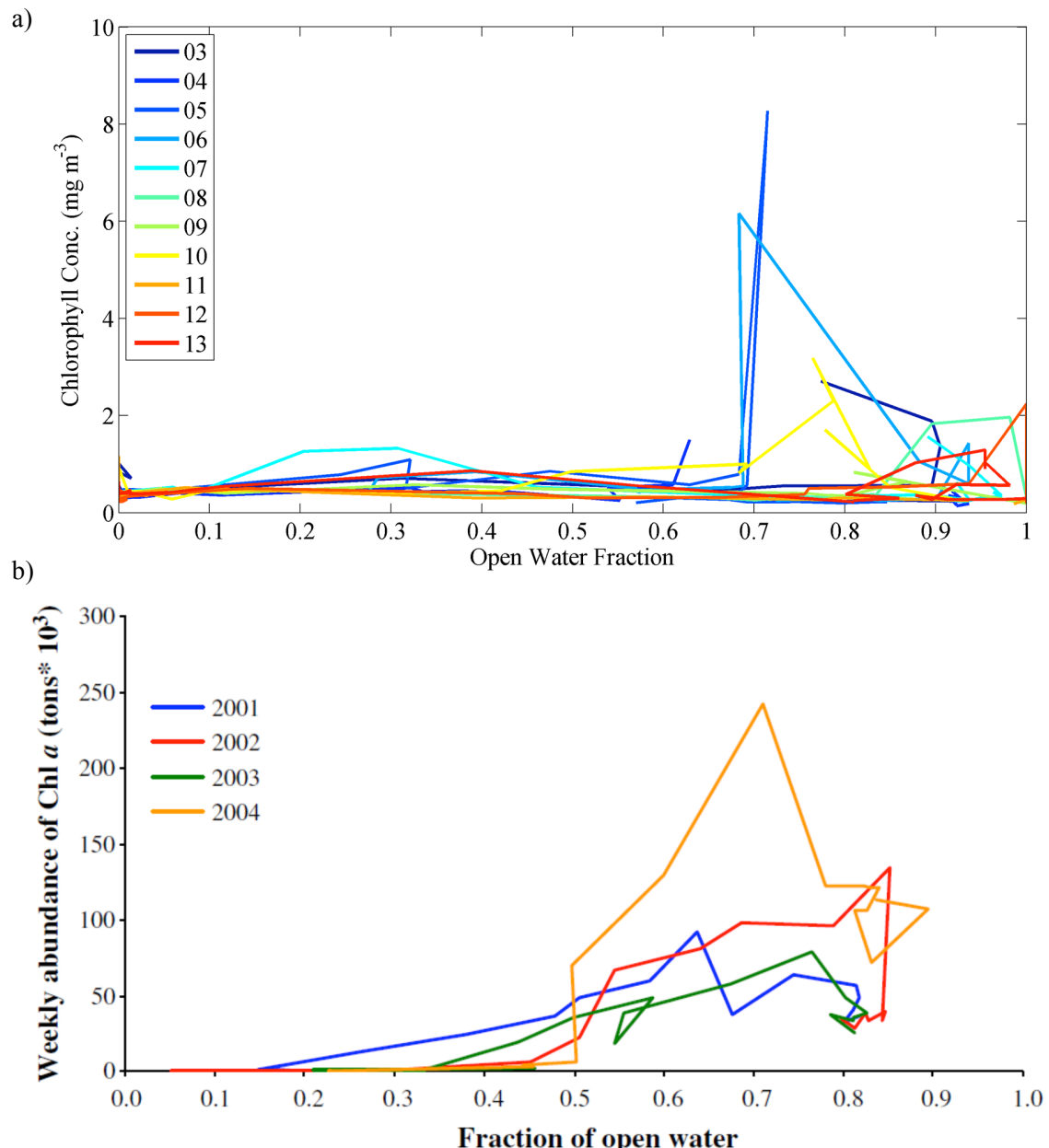


**Fig. 19.** (a) open water fraction vs. chlorophyll concentration 2003-2013 over the Baffin Shelf. Data from mini-box method. (b) open water fraction vs. abundance of chlorophyll 2001-2004 in Disko Bay, West Greenland [lower panel figure taken from Heide-Jorgensen et al. (2007), p. 91].

period were also the highest of all years ( $7.71 \text{ m s}^{-1}$ ), and had a stronger east component compared to the more northerly winds in most other years (see Fig. 13). High wind in some Arctic coastal polynyas such as the Chukchi Sea can be effective at diverging forming ice fields, promoting heat loss from the ocean during winter and generating high rates of sea ice production (Tamura et al., 2008; Ito et al., 2015). Results here contradict this. Instead, the stronger east component appeared to reduce the flux of cooler Arctic air, increasing air temperatures (see Fig. 14) which in turn may have reduced the effectiveness of ice formation over the shelf. The higher fraction of open water coupled with the high wind speed may have enhanced wind driven mixing of surface waters (Hunt et al., 2002; Arrigo & Dijken., 2004; Sullivan et al., 2014), despite a reduction in convective mixing from sea ice brine rejection (Carmack & Macdonald, 2002).

The lower magnitude of sea ice concentration after  $t_{ice}(Gaus)$  would naturally lead to smaller volumes of iron rich meltwater (Wang et al., 2014), which may have been directly entrained due to high wind shear (Arrigo & Dijken, 2004; Stabeno et al., 2010). A lack of haline stratification and turbulent mixing in 2005 may have resulted in phytoplankton being mixed below the euphotic layer where light limiting conditions prevent an early bloom (Harrison & Li, 2007). Therefore, this bloom could be attributed to more traditional bloom mechanisms, such as the shutdown or relaxation of turbulent convection and mixing (Townsend et al., 1992; Huisman et al., 1999; Chiswell, 2011; Taylor & Ferrari, 2011).

### 6.3. Impacts of Sea Ice Retreat Driven Blooms on the Labrador Sea Ecosystem

The potential implications of sea ice dynamics on marine food web and community structure as a whole is becoming of increasing concern. Sea ice loss has emerged as a critical driver to

marine and terrestrial productivity, influencing species interactions, population mixing, gene flow, and pathogen and disease transmission (Post et al., 2013). On the Newfoundland-Labrador Shelf, Fuentes-Yaco et al. (2007) identifies significant correlation between phytoplankton bloom intensity, timing of the maximum and bloom duration to the size of young shrimp (*Pandalus borealis*). Here the success of the shrimp is controlled by the availability of food, with the spring bloom being a valuable source (Fuentes-Yaco et al., 2007). Wu et al. (2007) show spring bloom dynamics here are strongly linked to the annual retreat of sea ice. Together this emphasises the influence of ice dynamics on the marine community beyond primary producers. Naturally, a mismatch between the bloom and the reproductive cycle of secondary producers would negatively influence higher trophic levels of the food web in its existing form (Kahru et al., 2011). This is particularly important for the Labrador Sea, which contains a relatively short, efficient food chain where large secondary producers (e.g. *Calanus* copepod) graze directly on the phytoplankton (Frajka-Williams & Rhines, 2010). Tertiary predators then heavily exploit the *Calanus*, which in turn attracts the bowhead whale between February and May of each year (Laidre et al., 2007).

Arrigo & Dijken (2004) suggest blooms that develop in cold surface water are bottom-up controlled due to resource limitation, rather than top-down controlled due to low grazing rates at low temperatures. In this case, fluxes of energy and carbon are more heavily weighted to benthic communities, negatively impacting food availability to the pelagic consumers (Stabeno et al., 1998; Hunt et al., 2002). On the eastern Bering Sea Shelf, shifts between top-down and bottom-up control in food webs have been shown to affect commercially harvestable fish stocks such as Pollock (Hunt et al., 2002). It is unknown if a similar feedback may exist in the Labrador Sea, however, Fuentes-Yaco et al. (2007) and

Koeller et al. (2007) have shown that inter-annual fluctuations in the characteristics of the spring bloom in the Arctic and sub-Arctic are significant for higher trophic levels, including harvestable stocks. Ji et al. (2013) and Leu et al. (2011) emphasise zooplankton grazers across the Arctic are most affected by phytoplankton production variability, which again is often strongly controlled by sea ice dynamics (e.g. Wu et al., 2007; Jin et al., 2012).

We can assume interannual variation in ice extent and time of ice retreat over the Baffin Shelf is likely to be important for ecosystem dynamics of the Labrador Sea, with wider implications for ocean biogeochemical cycling (Sedwick & DiTullio, 1997; Ducklow et al., 2012). Increased frequency of short and intensive phytoplankton bloom events in the future, and longer periods of open water during the summer may lead to a shift towards smaller phytoplankton species and alter biogeochemical cycling (Li et al., 2009; Fujiwara et al., 2014). An overall reduction in phytoplankton biomass would negatively influence the food web including commercially harvestable species. Further, a shift in the relative amount of primary production in an under-ice bloom (if present) vs. ice-edge bloom environment may either positively or negatively affect total ecosystem productivity, particularly the benthic food web (Palmer et al., 2014).

### 6.4. Method Selection

The mini-box method was the only method to identify a strong coupling between sea ice retreat and the onset of the spring phytoplankton bloom over the Baffin Shelf. With three other methods producing no statistically meaningful coupling, one could argue that a null result is more likely to exist in reality, and that the reliability of the strong coupling identified is reduced by the other null results.

To maintain an element of consistency between methods, computations of  $t_{ice}(Gaus)$  and  $t_{sb}(onset)$  remained consistent once a time series for sea ice concentration and chlorophyll had been obtained. For each method, Gaussian fitting and computations of  $t_{ice}(Gaus)$  and  $t_{sb}(Gaus)$  were checked to ensure fitting and estimates were sensible and appropriate to the relevant time series. Therefore, differences in results originate from the initials steps required to obtain these time series, prior to computations of  $t_{sb}(onset)$  and  $t_{ice}(Gaus)$ . The mini-box method was most straight forward, requiring a single step of spatial averaging within its confines to produce the relevant time series. By averaging in this way, the method gave no spatial bias to density or magnitude of chlorophyll pixels. Despite the relatively high latitude and compact study area, the volume of chlorophyll data yielded was more than sufficient for this study. A minor amount of interpolation was required during 2004 and 2007 to counteract the effect of persistent cloud cover and produce a complete chlorophyll time series.

Despite covering approximately 50% of the mini-box area, the greater variation in latitude, depth range (Baffin Shelf to deep central water), and spatial coverage of the multi-transect method is assumed responsible for masking the coupling between sea ice retreat and the spring bloom over the Baffin Shelf. The length of the transects used meant their furthest extents were near the western coast of Greenland (see Fig. 3) where the north bloom occurs (Frajka-Williams & Rhines, 2010). Therefore, this method may be merging traces of both blooms. For example, Figure 15 shows significant chlorophyll during 2006 at 800 km along the transect, separate to chlorophyll activity near the ice edge. I suggest the coupling between sea ice retreat and the Baffin bloom is not absent from this method, rather it is diluted or masked by neighbouring physical and biological processes. In short, the spatial

coverage of this method is probably too large. A similar explanation is assumed responsible for null results from the large box method.

The single transect method could not be used to compute estimates of  $t_{ice}/t_{ice}(Gaus)$  and  $t_{sb}(onset)$ . The narrow width of the single transect meant instances of low data return due to cloud cover were common, and therefore estimates of  $t_{sb}(onset)$  could not be accurately computed. Further, Gaussian fitting and linear interpolation could not accurately represent the chlorophyll seasonal cycle due to the extent of missing data.

### 6.5. Mains Limitations & Future Work

#### *Limitations of L3 Satellite Chlorophyll Composites:*

Missing data due to cloud cover and other aerosols negatively impacted the quality and volume of chlorophyll data near the Baffin Shelf, despite using 8-day composites. Conservative use of linear interpolation aided the production of complete seasonal cycles. Estimates of  $t_{sb}$  presented in the relevant panels in Figure 9 were only made possible by regridding chlorophyll to 25 km to reduce the impact of patchy cloud cover.

Here chlorophyll data has been used to infer abundance of phytoplankton during ice retreat. Chlorophyll is regarded as a proxy for phytoplankton abundance (Huot et al., 2007) and does not represent abundance of the entire water column (Robinson, 2010). Further, these variables are only considered as a proxy for primary production (Huot et al., 2007). For example, a high concentration of chlorophyll or phytoplankton cells does not guarantee high production if cells are resource (light or nutrient) limited (Hickman et al., 2012). For the purposes of this report, chlorophyll results are deemed sufficiently reliable to make realistic conclusions regarding phytoplankton dynamics and primary production.

### ***Limitations of Satellite Sea Ice Concentration Composites:***

Sea ice data near coastlines was particularly noisy, where the seasonal and annual cycle was often totally obscured (not shown). This was most prominent along the west Greenland coast. Noisy data was confined to the shallowest regions of most coastlines, with data further offshore being un-affected.

### ***Limitations of Analysis:***

This study did not fit Gaussian curves to chlorophyll data. Although the onset of the bloom was of most interest to this study, obtaining additional bloom parameters (e.g. bloom duration) from a fitted curve (as in Wu et al., 2007) may have aided quantification of Baffin bloom climatology. Gaussian fitting to the sea ice concentration time series was necessary to remove somewhat erratic behaviour of the seasonal cycle. Whilst this led to sensible estimates of  $t_{ice}(Gaus)$ , it could be argued a simple moving average (e.g. 20 day) may have produced a more representative fit and therefore more appropriate than Gaussian fitting.

### ***Future Work:***

A brief preliminary analysis of chlorophyll and sea ice concentration composites across the northern hemisphere is presented in Figure 20. The figure was created to help find new regions where sea ice may influence the development of the spring bloom. Based on the anomaly computations of  $t_{sb}(onset)$  and  $t_{ice}(50\%)$  in the figure, a number of regions exhibited visually similar sea ice-plankton dynamics to those observed in the Labrador Sea, for example: Hudson Bay ( $60^{\circ}\text{N}$ ,  $90^{\circ}\text{W}$ ), Greenland Sea ( $75^{\circ}\text{N}$ ,  $15^{\circ}\text{W}$ ), and the Sea of Okhotsk ( $55^{\circ}\text{N}$ ,  $140^{\circ}\text{W}$ ). Future studies may wish to focus on these regions, subjecting them to a more stringent investigation than the preliminary computations shown here.

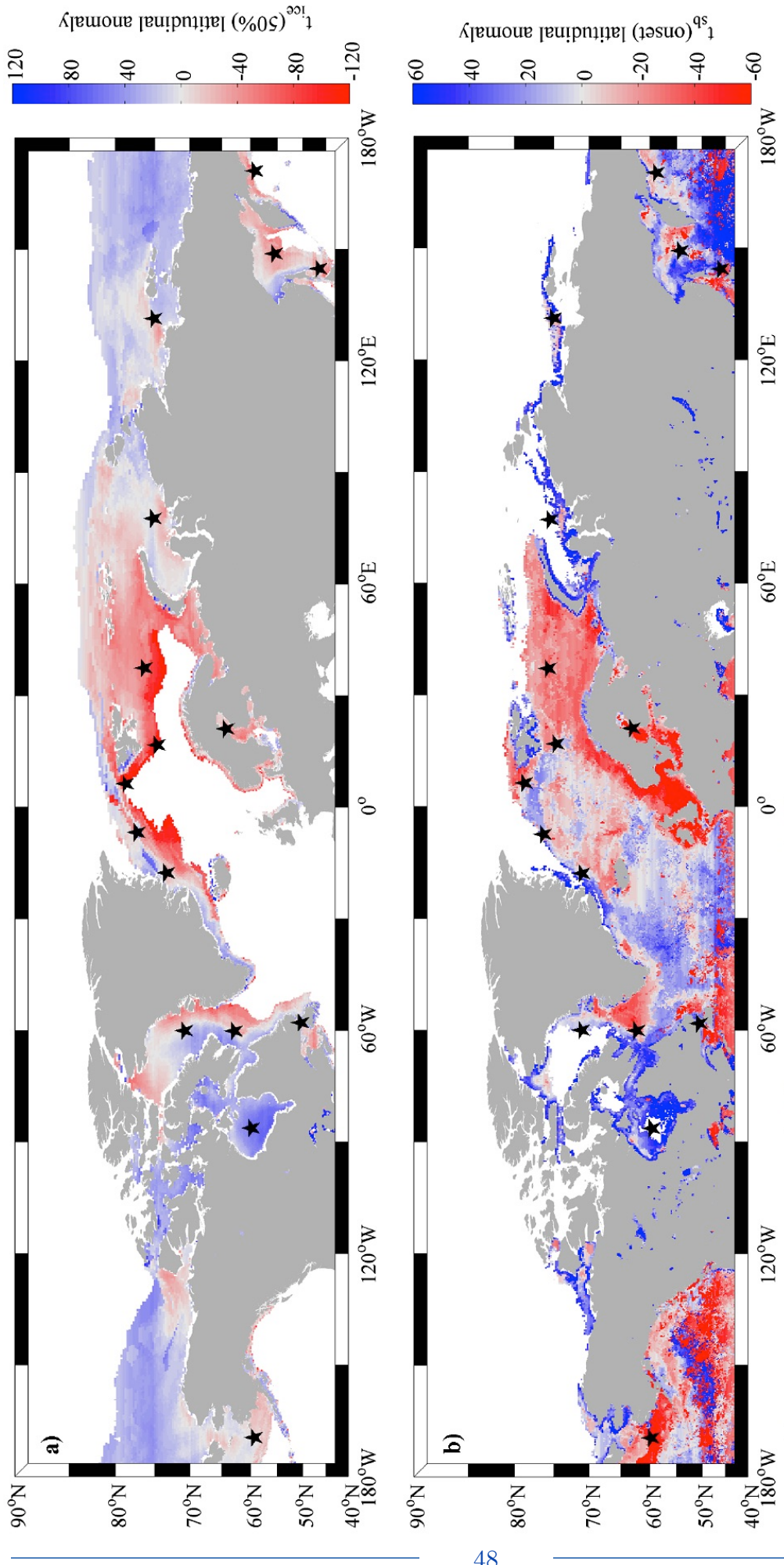


**Fig. 20.** (a): Latitudinal anomalies of  $t_{ice}(50\%)$  for 2003-2013, where  $t_{ice}(50\%)$  was computed using the method described in Section 4.1. Anomalies calculated by subtracting the latitude average of  $t_{ice}(50\%)$  from estimates at each 25 km grid point. White areas indicate regions of open water or permanent ice cover.

(b): Latitudinal anomalies of  $t_{sb}(onset)$  for 2003-2013, where  $t_{sb}(onset)$  was also computed using the method described in Section 4.1. Anomalies calculated by subtracting the latitude average of  $t_{sb}(onset)$  from individual estimates at each 25 km grid point. White areas indicate regions of no data. *General:* red shades indicate areas where sea ice retreat or the onset of the spring bloom occurs early for its latitude, and blue shades indicate lateness for the given latitude (expressed as day number). Black stars indicate regions of comparable anomalies between panels, where sea ice retreat may be responsible for the onset of the bloom.

## 7. Conclusion

The observations reported here add to the increasing evidence that sea ice dynamics may influence the onset of the spring bloom in Arctic and sub-Arctic regions. During the 2003-2013 period considered here, a strong correlation of 0.7 between sea ice retreat and the onset of the bloom was identified over the Baffin Shelf, significant at the 95% confidence interval. The causation and climatological variations in the timing of the Baffin bloom is attributed to light limitation due to sea ice cover. Haline stratification may also play an important role in the magnitude and duration of the bloom. During the winter-spring period of 2005, the highest wind speeds and warmest air temperatures of the study period coincided with the lowest sea ice concentrations. High wind speed did not enhance ice formation, contrary to findings in other studies. Instead, the warm air temperatures likely hampered its development, and led to its rapid retreat. Ultimately, the lack of sea ice cover and strong winds may have led to enhanced turbulent mixing of the water column, delaying the onset of the bloom compared to other years. The delay did not adversely effect the general correlation between sea ice retreat and the development of the bloom identified. However, one must consider that the 2005 spring bloom could be attributed to more traditional formation theory, such as the seasonal shutdown (or relaxation) of turbulent mixing.

Additional methods explored failed to identify a strong correlation in sea ice-plankton dynamics. Their lack of success is attributed to their broad spatial coverage, where the trend of interest may be masked by the influence of neighbouring physical and biological processes. Confidence in the mini-box method is greater due to its spatial confinement and straight forward approach, where only one stage of processing is required to produce a linear time

series of sea ice concentration and chlorophyll concentration. Gaussian fitting produced sensible estimates for ice retreat timing in this study. However, a comparison of different fitting techniques in the future may be useful to this area of research.

Motivation of this study stemmed from the critical ecological value existing spring blooms in the Labrador Sea have on the ecosystem. Existing studies suggest the reproductive cycles of secondary consumers are tuned to the timing of spring blooms over the Labrador and Newfoundland shelves. Therefore, a mismatch between primary and secondary consumers may prove detrimental to the short, efficient food chain. A lack of research and documentation of this bloom suggest current primary production estimates for the Labrador Sea are underestimated. Reducing sea ice coverage in the future may have several and potentially irreversible implications to the Labrador Sea ecosystem. Future work should focus on expanding research into the causation of blooms in seasonally ice cover regions. Further, we should seek a better understanding on the ecological value of sea ice induced spring blooms, including their implications for ocean biogeochemistry, ecosystem functionality, and what changes to expect in the future.

## 8. References

- Ardyna, M. et al. (2014). Recent Arctic Ocean sea ice loss triggers novel fall phytoplankton blooms. *Geophysical Research Letters* 41, 6207-6212.
- Arrigo, K.R. & van Dijken, G.L. (2004). Annual cycles of sea ice and phytoplankton in Cape Bathurst polynya, southeastern Beaufort Sea, Canadian Arctic. *Geophysical Research Letters* 31 (L08304).
- Arrigo, K.R. et al. (2012). Massive phytoplankton blooms under Arctic sea ice. *Science* 336, p. 1408.
- Barber, D.G. & Massom, R.A. (2007). Chapter 1: The role of sea ice in Arctic and Antarctic polynyas. *Elsevier Oceanography Series* 74, 1-54.
- Behrenfeld, M.J. (2010). Abandoning Sverdrup's critical depth hypothesis on phytoplankton blooms. *Ecology* 91, 977-989.
- Berrisford, P. et al. (2011). The ERA-Interim archive Version 2.0. ERA Report Series (1), European Centre for Medium Range Weather Forecasts, UK. Available from: <http://www.ecmwf.int/en/forecasts/datasets/era-interim-dataset-january-1979-present>
- Carmack, E.C. & Macdonald, R.W. (2002). Oceanography of the Canadian Shelf of the Beaufort Sea: A setting for marine life. *Arctic* 55, 29-45.
- Carmack, E.C., Macdonald, R.W., Jasper, S. (2004). Phytoplankton productivity on the Canadian Shelf of the Beaufort Sea. *Marine Ecological Progress Series* 277, 37-50.
- Chiswell, S.M. (2011). Annual cycles and spring blooms in phytoplankton: don't abandon Sverdrup completely. *Marine Ecology Progress Series* 443, 39-50.
- Cushing, D.H. (1959). The seasonal variation in oceanic production as problem in population dynamics. *Journal du Conseil International pour l'Exploration de la Mer* 24, 455-464.
- Ducklow, H.W., Schofield, O., Vernet, M., Stammerjohn, S., Erickson, M. (2012). Multiscale control of bacteria production by phytoplankton dynamics and sea ice along the western Antarctic Peninsula: A regional and decadal investigation. *Journal of Marine Systems* 98/99, 26-39.
- Eilertsen, H.C. (1993). Spring blooms and stratification. *Nature* 363, 24.
- Fischer, A.D. et al. (2014). Sixty years of Sverdrup: A retrospective of progress in the study of phytoplankton blooms. *Oceanography* 27(1), 222-235.
- Frajka-Williams, E. & Rhines, P.B. (2010). Physical controls and Interannual variability of the Labrador Sea spring phytoplankton bloom in distinct regions. *Deep-Sea Research I* 57, 541-552.
- Frajka-Williams, E., Rhines, P.B., Eriksen, C.C. (2009). Physical controls and mesoscale variability in the Labrador Sea spring phytoplankton bloom observed by Seaglider. *Deep-Sea Research I* 56, 2144-2161.
- Fuentes-Yaco, C., Koeller, P.A., Sathyendranath, S., Platt, T. (2007). Shrimp (*Pandalus borealis*) growth and timing of the spring phytoplankton bloom on the Newfoundland-Labrador Shelf. *Fisheries Oceanography* 16(2), 116-129.
- Fujiwara, A., Hirawake, T., Suzuki, K., Imai, I., Saitoh, S.I. (2014). Timing of sea ice retreat can alter phytoplankton community structure in the western Arctic Ocean. *Biogeosciences* 11, 1705-1716.
- Hansen, A.S. et al. (2002). Impact of changing ice cover on pelagic productivity and food web structure in Disko Bay, West Greenland: a dynamic model approach. *Deep-Sea Research I* 50, 171-187.
- Harrison, W.G. & Li, W.K.W. (2007). Phytoplankton growth and regulation in the Labrador Sea: Light and nutrient limitation. *Journal of Northwest Atlantic Fisheries Science* 39, 71-82.
- Head, E.J.H., Harris, L.R., Campbell, R.W. (2000). Investigations on the ecology of *Calanus* spp. in the Labrador Sea. I. Relationship between the phytoplankton bloom and reproduction and development of *Calanus finmarchicus* in spring. *Marine Ecology Progress Series* 193, 53-73.
- Heide-Jørgensen, M.P., Laidre, K.L., Logsdon, M.L., Nielsen, T.G. (2007). Springtime coupling between chlorophyll a, sea ice and sea surface temperature in Disko Bay, West Greenland. *Progress in Oceanography* 73, 79-95.
- Hickman, A.E. et al. (2009). Distribution and chromatic adaptation of phytoplankton within a shelf sea thermocline. *Limnology and Oceanography* 54, 525-536.
- Hickman, A.E., et al. (2012). Primary production and nitrate uptake within the seasonal thermocline of a stratified shelf sea. *Marine Ecology Progress Series* 463, 39-57.
- Huisman, J.P., van Oostveen, P., Weissing, F.J. (1999). Critical depth and critical turbulence: Two different mechanisms for the development of

- phytoplankton blooms. *Limnology and Oceanography* 44, 1781-1787.
- Hunt, G.L., Stabeno, P.J., Walters, G., Sinclair, E., Brodeur, R.D., Napp, J.M., Bond, N.A. (2002). Climate change and control of the south-eastern Bering Sea pelagic ecosystem. *Deep-Sea Research II* 49, 5821-5853.
- Huot, Y., Babin, M., Bruyant, F., Grob, C., Twardowski, M.S., Claustre, H. (2007). Does chlorophyll a provide the best index of phytoplankton biomass for primary productivity studies? *Biogeosciences Discussions* 4, 707-745.
- Ito, M. et al. (2015). Observations of supercooled water and frazil ice formation in an Arctic coastal polynya from moorings and satellite imagery. *Annals of Glaciology* 56(69), 307-314.
- Ji, R., Jin, M., Varpe, O. (2013). Sea ice phenology and timing of primary production pulses in the Arctic Ocean. *Global Change Biology* 19, 734-741.
- Jin, M., Deal, C., Lee, S.H., Elliott, S., Hunke, E., Maltrud, M., Jeffery, N. (2012). Investigation of Arctic sea ice and ocean primary production for the period 1992-2007 using a 3-D global ice-ocean ecosystem model. *Deep-Sea Research II* 81-84, 28-35.
- Juul-Pedersen, T. et al. (2006). Sedimentation following the spring bloom in Disko Bay, West Greenland, with special emphasis on the role of copepods. *Marine Ecology Progress Series* 314, 239-255.
- Kahru, M., Brotas, V., Manzano-Sarabia, M., Mitchell, B.G. (2011). Are phytoplankton blooms occurring earlier in the Arctic? *Global Change Biology* 17, 1733-1739.
- Koeller, P., Fuentes-Yaco, C., Platt, T. (2007). Decreasing shrimp sizes off Newfoundland and Labrador – environment or fishing? *Fisheries Oceanography* 16(2), 105-115.
- Laidre, K.L., Heide-Jorgensen, M.P., Nielsen, T.G. (2007). Role of the bowhead whale as a predator in west Greenland. *Marine Ecology Progress Series* 346, 285-297.
- Laidre, K.L., Heide-Jorgensen, M.P., Nyeland, J., Mosbech, A., Boertmann, D. (2008). Latitudinal gradients in sea ice and primary production determine Arctic seabird colony size in Greenland. In: *Proceedings of the Royal Society B* 275, 2695-2702.
- Leu, E., Soreide, J.E., Hessen, D.O., Falk-Petersen, S., Berge, J. (2011). Consequences if changing sea-ice cover for primary and secondary producers in the European Arctic shelf seas: Timing, quantity, and quality. *Progress in Oceanography* 90, 18-32.
- Li, W.K.W., McLaughlin, F.A., Lovejoy, C., Carmack, E.C. (2009). Smallest algae thrive as the Arctic Ocean freshens. *Science* 326(5952), p. 539.
- Mahiny, S.A., Fendereski, F., Hosseini, S.A., Fazli, H. (2013). A MODIS-based estimation of chlorophyll a concentration using ANN model and in-situ measurements in the southern Caspian Sea. *Indian Journal of Geo-Marine Sciences* 42(7), 924-928.
- Nielsen, T.G. & Hansen, B. (1999). Plankton structure and carbon cycling on the western coast of Greenland during the stratified summer situation. I. Hydrography, phytoplankton, and bacterioplankton. *Aquatic Microbiological Ecology* 16, 205-216.
- O'Reilly, J.E. et al. (2000). Ocean color chlorophyll a algorithms for SeaWiFS, OC2, and OC4: Version 4. In: O'Reilly, J.E. and 24 co-authors, 2000: SeaWiFS Postlaunch Calibration and Validation Analyses, Part 3. NASA Tech. Memo. 2000-206892, Vol. 11, S.B. Hooker and E.R. Firestone, Eds., NASA Goddard Space Flight Center, Greenbelt, Maryland, 9-23.
- Okubo, A. (1980). *Diffusion and Ecological Problems: Mathematical Models*. Springer-Verlag, Berlin-Heidelberg-New York, p. 254.
- Palmer, M.A., Saenz, B.J., Arrigo, K.R. (2014). Impacts of sea ice retreat, thinning, and melt-pond proliferation on the summer phytoplankton bloom in the Chukchi Sea, Arctic Ocean. *Deep-Sea Research II* 105, 85-104.
- Pedersen, S.A., Kanneworf, P. (1995). Fish on the West Greenland shrimp grounds, 1988-1992. *Journal of Marine Science* 52, 165-182.
- Post, E. et al. (2013). Ecological consequences of sea-ice decline. *Science* 341, 519-524.
- Robinson, I.S. (2010). *Discovering the Ocean from Space*. Springer Berlin Heidelberg: UK.
- Sandwell, D.T. (1991). Geophysical applications of satellite altimetry. *Reviews of Geophysics*, Supplement, p. 132-137. In: U.S. National Report to International Union of Geodesy and Geophysics 1987-1990.
- Schandelmeier, L. & Alexander, V. (1981). An analysis of the influence of ice on spring phytoplankton population structure in the southeast Bering Sea. *Limnology and Oceanography* 26(5), 935-943.
- Sedwick, P.N. & DiTullio, G.R. (1997). Regulation of algal blooms in Antarctic shelf waters by the release of iron from melting sea ice. *Geophysical Research Letters* 24, 2515-2518.
- Siegal, D., Doney, S., Yoder, J. (2002). The North Atlantic spring phytoplankton bloom and Sverdrup's critical depth hypothesis. *Science* 296, 730-733.

- Smetacek, V. & Passow, U. (1990). Spring bloom initiation and Sverdrup's critical-depth model. *Limnology and Oceanography* 35, 228-234.
- Smith, S.D., Muench, R.D., Pease, C.H. (1990). Polynyas and leads: An overview of physical processes and environment. *Journal of Geophysical Research* 95, 9461-9479.
- Stabeno, P.J., Bond, N.A., Kachel, N.B., Salo, S.A., Schumacher, J.D. (2001). On the temporal variability of the physical environment over the southeastern Bering Sea. *Fisheries Oceanography* 10, 81-98.
- Stabeno, P.J., Napp, J., Mordy, C., Whitledge, T. (2010). Factors influencing physical structure and lower trophic levels of the eastern Bering Sea shelf in 2005: Sea ice, tides and winds. *Progress in Oceanography* 85(3-4), 180-196.
- Stabeno, P.J., Schumacher, J.D., Davis, R.F., Napp, J.M. (1998). Under-ice observations of water column temperature and spring phytoplankton dynamics: Eastern Bering Sea Shelf. *Marine Research* 56, 239-255.
- Staehr, P.A. & Sandjensen, K. (2005). Seasonal changes in temperature and nutrient control of photosynthesis, respiration and growth of natural phytoplankton communities. *Freshwater Biology* 51(2), 249-262.
- Sullivan, M.E. et al. (2014). Sea ice and water column structure on the eastern Bering Sea shelf. *Deep-Sea Research II* 109, 39-56.
- Sverdrup, H.U. (1953). On conditions for the vernal blooming of phytoplankton. *Journal du Conseil International pour l'Exploration de la Mer* 18, 287-295.
- Tamura, T., Ohshima, K.I., Nihashi, S. (2008). Mapping of sea ice production for Antarctic coastal polynyas. *Geophysical Research Letters* 35(7), L07606.
- Taniguchi, A., Saito, K., Koyama, A., Fukuchi, M. (1976). Phytoplankton communities in the Bering Sea and adjacent Seas. *Journal of Oceanography* 32(3), 99-106.
- Taylor, J. & Ferrari, R. (2011). Shutdown of turbulent convection as a new criterion for the onset of spring phytoplankton blooms. *Limnology and Oceanography* 56, 2293-2307.
- Townsend, D.W., Keller, M.D., Sieracki, M.E., Ackleson, S.G. (1992). Spring phytoplankton blooms in the absence of vertical water column stratification. *Nature* 360, 59-62.
- Wang, S., Bailey, D., Lindsay, K., Moore, J.K., Holland, M. (2014). Impact of sea ice on the marine iron cycle and phytoplankton productivity. *Biogeosciences* 11, 4713-4731.
- Wu, Y. et al. (2007). The impact of sea ice on the initiation of the spring bloom on the Newfoundland and Labrador Shelves. *Journal of Plankton Research* 29(6), 509-514.
- Wu, Y., Platt, T., Tang, C.C.L., Sathyendranath, S. (2008). Regional differences in the timing of the spring bloom in the Labrador Sea. *Marine Ecology Progress Series* 355, 9-20.
- Yoder, J. & McClain, C. (1993). Annual cycles of phytoplankton chlorophyll concentrations in the global ocean: A satellite view. *Global Biogeochemical Cycles* 7: 181-193.
- Zhang, J. et al. (2010). Modelling the impact of declining sea ice on the Arctic marine planktonic ecosystem. *Journal of Geophysical Research* 115(C10015).